empirically determined by selecting the minimal time period for each step (1 or 2 h for fixation and three times 1 h for dehydration under gentle agitation), and analyses of molecules were performed usually within 1 month after paraffin embedding. However, we did not examine the effects of fixation and following dehydration periods or the storage time and temperature after paraffin embedding.

Determination of a suitable range for lengths of fixation/dehydration steps is very important for practical molecular analysis using methacarn if large numbers of tissue samples are to be analyzed, such as in the case of animal experiments requiring time-consuming autopsy. Furthermore, conditions for long-term storage of PETs for effective molecular analysis need to be optimized. The present study was therefore performed using methacarn-fixed and paraffin-embedded rat liver tissues from one animal with differing periods of processing and storage, focusing on the integrity of extracted molecules and the relative expression levels in sections.

Materials and methods

Chemicals and experimental animals

Sodium phenobarbital (PB) was purchased from Wako Pure Chemical Industries (Osaka, Japan). A 5-week-old CD (SD)IGS male rat from Charles River Japan Inc. (Atsugi, Japan) was maintained in an air-conditioned animal room (temperature 24 ± 1 °C, relative humidity 55 ± 5%) with a 12-h light/dark cycle and allowed ad libitum access to tap water and feed, CRF-1 (Oriental Yeast Co. Ltd., Tokyo, Japan). After 1-week acclimation, the rat was intraperitoneally injected with PB at 80 mg/kg body weight, once daily for 3 days. One day (24 h) after the last injection, the animal was killed by exsanguination from the abdominal aorta under deep anesthesia, and then the liver was removed for tissue processing. The dose was selected according to the PB-specific enzyme induction protocol described by Kocarek et al. [12], and the animal protocol was reviewed and approved by the Animal Care and Use Committee of the National Institute of Health Sciences, Japan.

Tissue preparation and storage

From the center portion of the left lobe, tissue blocks sized 5 × 5 × 3 mm were excised and subjected either to embedding in Tissue-Tek 4583 OCT compound (Sakura Finetek Japan, Tokyo, Japan) or to immersing in methacarn for tissue fixation. Methacarn solution consisting of 60% (vol/vol) absolute methanol, 30% chloroform, and 10% glacial acetic acid was freshly prepared and stored at 4 °C before fixation [5,7,9]. UFTs were quickly frozen in ethanol/dry ice and stored at −80 °C until sectioning on the next day after embedding. To examine the effects of length of time of tissue processing (Experiment 1), fixation with methacarn and subsequent dehydration with 99.5% ethanol were performed for 2 and 16 h (overnight), 5 and 16 h, 16 and 16 h, or 2 h and 1 week at 4 °C in a refrigerator. Tissue blocks were dehydrated twice in fresh ethanol solution for 1 h and then for 16 h (overnight) or 1 week. They were then paraffin embedded as described previously [9], and tissue sectioning was performed within 1 week after paraffin embedding. To examine PET storage conditions (Experiment 2), 2 h-fixed overnight-dehydrated tissues were stored for 1 month at 4 °C or 3 or 12 months either at 4 °C in a refrigerator or at room temperature in a laboratory. Both UFTs and PETs were sectioned at 10 μm and a total of 20 sections per block were collected in 1.5-ml microtubes for storage at −80 °C until extraction of molecules.

RNA analysis

Methacarn-fixed PET sections stored at −80 °C were subjected to deparaffinization with xylene three times for 5 min, immersed in 100% ethanol three times for 5 min, and immediately processed for RNA extraction using an RNeasy Mini kit (Qiagen GmbH, Hilden, Germany) according to the manufacturer's protocol. For UFT sections stored at −80 °C, total RNAs were immediately extracted after removal from the deep freezer. The final elution volume was set at 30 μl and contaminating genomic DNA was digested with DNase I (Ambion, Austin, TX) according to the manufacturer's protocol. For quantitation of RNA yield, 1 μl of isolated RNA was labeled with a RiboGreen RNA Quantitation kit (Molecular Probes, Eugene, OR) and concentrations were estimated with a fluorescence spectrophotometer F2500 (Hitachi Co. Ltd., Tokyo, Japan) in 1 ml of total volume with water [5]. To examine the integrity of 18S and 28S ribosomal RNAs in the extracted total RNAs, 1 μg from each sample was loaded onto a 1.0% agarose gel and visualized with ethidium bromide. The integrity was also examined by measuring the 28S/18S ribosomal RNA ratio with an RNA 6000 Nano LabChip kit (Agilent Technologies, Mountain View, CA) and RNA ladders (Ambion) in an Agilent 2100 bioanalyzer according to the manufacturer's directions.

For measurement of relative mRNA expression levels, the following four mRNA species were selected: cytochrome P450 (CYP) 2B1 (GenBank/EMBL Data Bank, Accession No. M37134), glyceraldehyde-3-phosphate dehydrogenase (GAPDH; Accession No. M17701), solute carrier family 34A2 (slc34a2; Accession No. NM_053380.1), and syntaxin 6 (stx6; Accession No. NM_031665.1). CYP2B1 is a gene that is known to show strong induction in the liver by PB treatment of rats [9], and GAPDH is a representative housekeeping gene. Slc34a2 and stx6 were found to show specific expression changes by microarray analysis at the tumor promotion stage in the experimental hepatocarcinogenesis study previously performed in our laboratory using rats, and their expression levels relative to that of GAPDH were found to be rather minor by real-time RT-PCR analysis (data not shown). For measurement of GAPDH and CYP2B1 mRNA levels, one-step real-time RT-PCR with the SYBR Green detection system was performed using the

ABI PRISM 7000 Sequence Detection System (Applied Biosystems Japan, Tokyo, Japan) in a 50-μl total reaction volume including 50 ng of total RNA, 300 nM each forward and reverse primers, 12.5 U Multiscribe Reverse Transcriptase, 10 U RNase Inhibitor, and 25 μl SYBR Green PCR Master Mix, according to the manufacturer's protocol (all reagents were purchased from Applied Biosystems Japan). Primer sets for both genes were identical with those used in our previous study [9]. Cycle parameters in this system were as follows: single step of 48 °C for 30 min, single step of 95 °C for 10 min, and 50 cycles of 95 °C for 15 s followed by 60 °C for 1 min. As for measurement of mRNA levels of slc34a2 and stx6, two-step real-time RT-PCR with the TaqMan probe detection system was performed. Gene-specific primers and the corresponding TaqMan MGB probes (6-FAM-dye-labeled) were derived from TaqMan Gene Expression Assays (Applied Biosystems Japan Ltd.). Reverse transcription was performed using 1 μg of total RNA with a High-capacity cDNA Archive Kit (Applied Biosystems Japan Ltd.) in a 100-μl total reaction volume. Real-time PCR was performed in a 50-μl reaction volume using the TaqMan probe detection system with 25 μl of TaqMan Universal PCR Master Mix (Applied Biosystems Japan Ltd.) and 2.5 μl each of target primer mix and reverse transcription product corresponding to 50 ng total RNA. Cycle parameters with this system were single step of 50 °C for 2 min, and initial activation at 95 °C for 10 min, and 50 cycles of 15 s at 95 °C and 60 s at 60 °C. Among real-time PCR methods, SYBR Green and TaqMan assays are known to produce comparable dynamic range and sensitivity [13]. For quantitation of expression data, a standard curve method was applied using the total RNA from UFTs as a standard sample.

Protein analysis

Deparaffinized sections were treated with 10% trichloroacetic acid in saline at 4 °C for 15 min. After brief centrifugation, pellets were washed once with ice-cold saline and then sonicated and solubilized in 200 μl of 2× sodium dodecyl sulfate (SDS) gel-loading buffer excluding bromophenol blue. Protein concentrations were estimated using a Nano-Orange Protein Quantitation Kit (Molecular Probes) and a fluorescence spectrophotometer [5]. After adjusting the protein concentration with 1× SDS gel-loading buffer including bromophenol blue, samples were heat-denatured at 80 °C for 30 min in the presence of 10% (v/v) β-mercaptoethanol and applied to 10% SDS polyacrylamide gel electrophoresis. For analysis of protein integrity, 20 μg of each protein extract was loaded, and resolved polypeptides were visualized after staining with 2.5% Coomassie brilliant blue. For Western blot analysis, resolved polypeptides were transferred to a polyvinylidine difluoride membrane (Millipore, Billerica, MA). Expression of three molecules with different functions and subcellular localizations were examined. After blocking with 0.2% casein, blots were incubated with either mouse monoclonal anti-β-actin (clone AC-15; Sigma; 20,000× in dilution), proliferating cell nuclear antigen (PCNA; clone PC10; Upstate, Charlottesville, VA; 1000× in dilution), or epidermal growth factor receptor (EGFR; clone 6F1; Medical and Biological Laboratories Co., Ltd., Nagoya, Japan; 300× in dilution) antibodies. Amounts of protein extract applied were 1 μg for β-actin, 5 μg for PCNA, and 15 μg for EGFR. As the secondary antibody, horseradish peroxidase-conjugated goat anti-mouse immunoglobulin (DakoCytomation Co., Ltd., Kyoto, Japan; 2000× in dilution) was used, and protein signals were detected with the ECL Western Blotting Detection System (Amersham Biosciences Corp., Piscataway, NJ). Relative protein levels of β-actin, PCNA, and EGFR were estimated by analyzing the band intensities using ONE-D/ZERO-Dscan Quantitative Gel and Blot Analysis software (Scanalytics, Inc., Fairfax, VA).

Statistical analysis

Comparison of 28S/18S ribosomal RNA ratios, yields of total RNA and protein, and expression levels of mRNA and protein retained in the tissues was performed with Student's *t* test when the variance was indicated to be homogeneous among groups using the test for equal variance. If a significant difference in the variance was observed, Welch's *t* test was performed. Comparison was first made between UFT and each PET preparation. In Experiment 1, comparisons were further performed between samples subjected to 2-h fixation/overnight dehydration or other fixation/dehydration conditions. Similar comparisons were also performed for Experiment 2. Variability was expressed as coefficient of variation (CV).

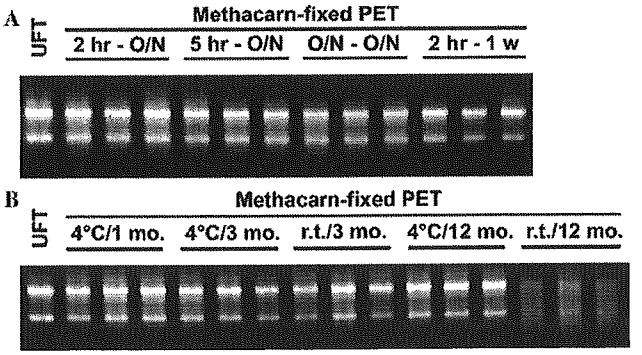

Fig. 1. Integrity of total RNAs extracted from methacarn-fixed rat liver PETs under different conditions of tissue processing or storage. One microgram of total RNA was applied to a 1% agarose gel and visualized with ethidium bromide. (A) Effects of period of tissue processing (Experiment 1): UFT, unfixed frozen tissue; 2 hr-O/N, samples fixed for 2 h followed by overnight dehydration; 5 hr-O/N, samples fixed for 5 h and dehydrated overnight; O/N-O/N, samples fixed overnight and then dehydrated overnight; 2 hr-1 w, samples fixed for 2 h and dehydrated for one week. (B) Storage effects of PETs with regard to period and temperature (Experiment 2): UFT, unfixed frozen tissue; 4 °C/1 mo., PETs stored for 1 month at 4 °C; 4 °C/3 mo., PETs stored for 3 months at 4 °C; r.t./3 mo., PETs stored for 3 months at room temperature; 4 °C/12 mo., PETs stored for 12 months at 4 °C; r.t./12 mo., PETs stored for 12 months at room temperature.

Results

Integrity and yield of total RNAs

In Experiment 1, integrity of total RNAs as judged by visual intensities for 18S and 28S ribosomal RNAs in agarose gel was not appreciably changed by the period of fixation up to overnight and dehydration up to 1 week (Fig. 1A). On measurement of the 28S/18S ribosomal RNA ratio, the integrity of total RNA was significantly reduced in methacarn-fixed PET sections compared with UFT sections (Table 1). The ribosomal RNA ratio remained unchanged from that of the 2-h fixed/overnight dehydrated case, although a tendency for reduction was observed in cases fixed for 5 h or overnight. Relative yields of total RNA per unit area were similar for all cases (Fig. 2A).

Table 1
28S/18S rRNA ratio of extracted total RNA in methacarn-fixed PETs under the different conditions for tissue processing or storage

Tissue condition	No. of samples	rRNA ratio [28S/18S][c]
Unfixed frozen	9	1.70 ± 0.45
Methacarn-fixed paraffin-embedded		
Fixation/dehydration[a]		
2 h/overnight	3	0.83 ± 0.07*
5 h/overnight	3	0.58 ± 0.04**
Overnight/overnight	3	0.62 ± 0.14**
2 h/1 week	3	0.70 ± 0.07**
Temperature/duration of storage[b]		
4 °C/1 month	6	0.75 ± 0.06**
4 °C/3 months	6	0.79 ± 0.09**
r.t./3 months	6	0.59 ± 0.14**
4 °C/12 months	6	0.66 ± 0.05**
r.t./12 months	6	Unmeasurable

*,**Significantly different from the unfixed frozen samples (*$p < 0.05$, **$p < 0.01$).

[a] Examination of the effect of time length for tissue processing (Experiment 1). Fixation and ethanol dehydration were performed at 4 °C. After dehydration, tissue blocks were paraffin embedded as described under Materials and methods. Already prepared PETs were stored at 4 °C until all of the tissues were processed for embedding.

[b] Examination of the effect of tissue storage with regard to the period and its temperature (Experiment 2). Fixation and ethanol dehydration were performed at 4 °C for 2 h and overnight, respectively. At the end of storage, tissue sections were prepared and stored at −80 °C until analysis.

[c] Data are expressed as mean ± SD.

In Experiment 2, when the visual integrity was compared among PET samples with different storage conditions, apparent reduction of both 18S and 28S ribosomal RNA bands was noted in samples stored for 12 months at room temperature (Fig. 1B), and this reduction resulted in the ribosomal RNA ratio being unmeasurable (Table 1). Although a nonsignificant reduction in the ribosomal RNA ratio was noted in PET samples stored for 3 months at room temperature as compared with those stored for 1 month at 4 °C, other PET storage conditions did not change the integrity of total RNA extracted (Fig. 1B, Table 1). Relative yields of total RNA per unit area were similar between the 1-month-stored case at 4 °C and each of the other cases (Fig. 2B).

Levels of mRNAs retained in PETs

On measurement of mRNA levels in PETs, mean threshold cycle (C_T: fractional cycle number at which the fluorescent signal passes the fixed threshold) of each gene was measured under the same input amount of total RNA using representative PET samples, i.e., 2-h-fixed/overnight-dehydrated samples in Experiment 1 and 1-month-stored samples at 4 °C in Experiment 2 (Table 2). As expected, C_T values of both GAPDH and PB-induced CYP2B1 were much smaller than those of slc34a2 and stx6, with ≥ 10-cycle differences simply reflecting ≥ 1000-fold expression differences. Judging from C_T values, relative quantity of transcripts was estimated to be in the order of CYP2B1 > GAPDH ≫ slc34a2 > stx6.

In Experiment 1, the GAPDH mRNA level retained in PETs was reduced in tissues dehydrated for 1 week to 62.2% of the 2-h-fixed/overnight-dehydrated case, but period of fixation did not affect the mRNA level (Fig. 3A). CYP2B1 mRNA levels were not apparently changed by the tissue-processing conditions. With regard to slc34a2, slight reduction of mRNA level was observed by 5-h fixation/overnight dehydration and 2-h fixation/1-week dehydration. Stx6 mRNA levels were not apparently changed irrespective of the fixation/dehydration conditions. With mRNA species examined, CV values ranged mostly within 20%, except for that of slc34a2 by overnight fixation being 40.0%.

In Experiment 2, retention of mRNAs in PETs was affected by storage for 12 months at room temperature, with reduction

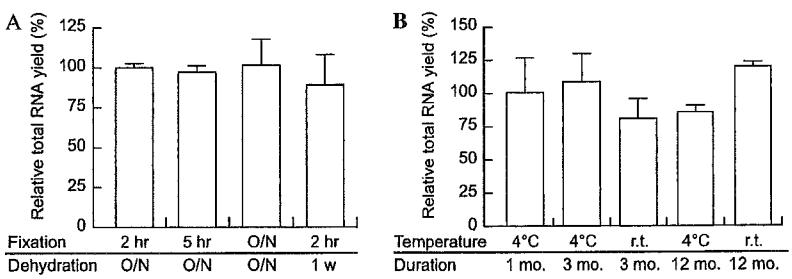

Fig. 2. Relative yields of total RNA in methacarn-fixed PETs under the different conditions of tissue processing or storage. (A) Experiment 1 ($n = 3$ for each condition). (B) Experiment 2 ($n = 6$ for each condition). Data are expressed as mean ± SD. Sample conditions were as for Fig. 1.

Table 2
Comparison of mean threshold cycle (C_T) of genes used in the present study in the methacarn-fixed paraffin-embedded rat liver tissue by real-time RT-PCR[a]

Tissue condition	No. of samples	Genes			
		GAPDH[b]	CYP2B1[b]	Slc34a2[c]	Stx6[c]
Fixation/dehydration[d]					
2 h/overnight	3	16.7	13.2	26.4	27.3
Temperature/duration of storage[e]					
4 °C/1 month	6	16.5	13.1	24.7	27.5

[a] Liver of a rat treated with PB for 3 days was used. C_T values in the 50 ng total RNA were measured at the fixed fluorescence threshold level of 0.14.
[b] Signal detection was performed by one-step real-time RT-PCR with the SYBR Green detection system.
[c] Signal detection was performed by two-step real-time RT-PCR with the TaqMan probe detection system.
[d] Examination of the effect of time length for tissue processing (Experiment 1). Already prepared PETs were stored at 4 °C until all of the tissues were processed for embedding.
[e] Examination of the effect of tissue storage with regard to the period and its temperature (Experiment 2). At the end of storage, tissue sections were prepared and stored at −80 °C until analysis.

of GAPDH, slc34a2, and stx6, to 76.1, 54.6, and 44.5%, respectively, of that for 1 month storage at 4 °C (Fig. 3B). Other storage conditions did not apparently affect the retention of mRNAs, while nonsignificant reduction was noted with slc34a2 stored for 3 months at 4 °C. CV values were mostly within 20%, except for those of slc34a2, ranging 21.3–33.8.

Integrity and yield of polypeptides

In Experiment 1, the visual pattern of resolved polypeptide bands and their intensities in polyacrylamide gels did not differ among samples with the tissue-processing conditions (Fig. 4A). However, protein yield was reduced in the 1-week dehydrated case as compared with that in the overnight dehydrated case after 2-h fixation (Fig. 5A).

In Experiment 2, the visual patterns of polypeptide bands were similar under the different storage conditions, but their intensities were rather reduced in the case of storage for 12 months at room temperature (Fig. 4B). With regard to protein yield, this was slightly reduced with storage of PETs at room temperature, reaching statistical significance in the 3-month storage case (Fig. 5B).

Levels of protein signals retained in PETs

In Experiment 1, retained levels of β-actin did not differ between the 2-h-fixed/overnight-dehydrated and other fixation/dehydration conditions, and variability in each was rather small (CV values <20%) (Fig. 6A). With PCNA, increase of relative expression was observed in samples fixed for 2 h and kept for 1 week at the dehydration step, the level being 132% of that with overnight dehydration, but the CV value was rather small (<20%) irrespective of the tissue-processing condition. In the EGFR case, a tendency for reduction of relative expression level was observed in 1-week-dehydrated PETs as compared with similar fixation for 2 h but dehydration overnight. However, this was not significant at least partly due to the variability in the expression values among samples in each condition, with CV values ranging 24.2–34.5%.

In Experiment 2, the retained expression level of β-actin was reduced in PETs stored at room temperature for more than 3 months, to 74% at 3 months and 52% at 12 months of the 1-month value at 4 °C (Fig. 6B). Slight, insignificant

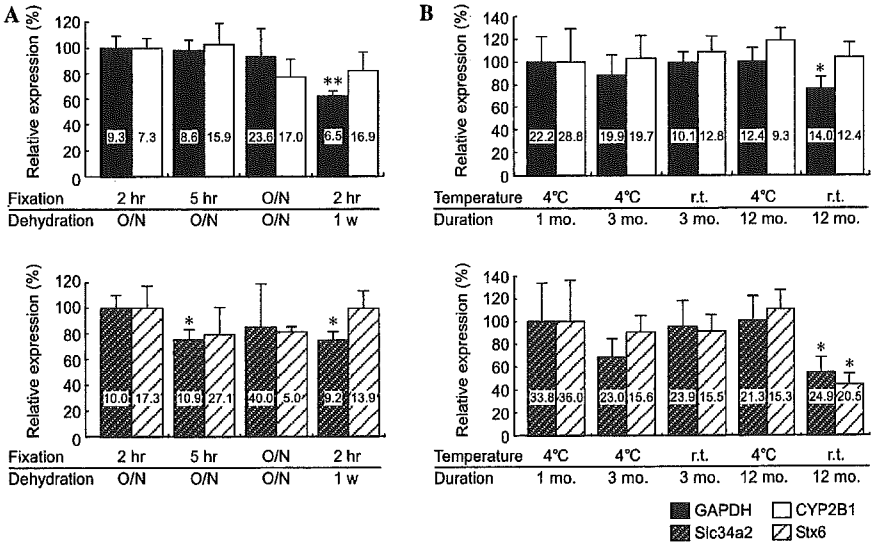

Fig. 3. Relative expression levels of GAPDH, CYP2B1, slc34a2, and stx6 mRNAs in methacarn-fixed PETs under the different conditions of tissue processing or storage. GAPDH and CYP2B1 mRNA levels were measured by one-step real-time RT-PCR with the SYBR Green detection system, and slc34a2 and stx6 mRNA levels were measured by two-step real-time RT-PCR with the TaqMan probe detection system. (A) Experiment 1 ($n = 3$ for each condition). (B) Experiment 2 ($n = 6$ for each condition). Data are mean ± SD values and coefficients of variation (CVs). *, **Significantly different from the 2-h-fixed/overnight-dehydrated case in Experiment 1, or from the 1-month-storage case at 4 °C in Experiment 2 ($^{*}p < 0.05$, $^{**}p < 0.01$).

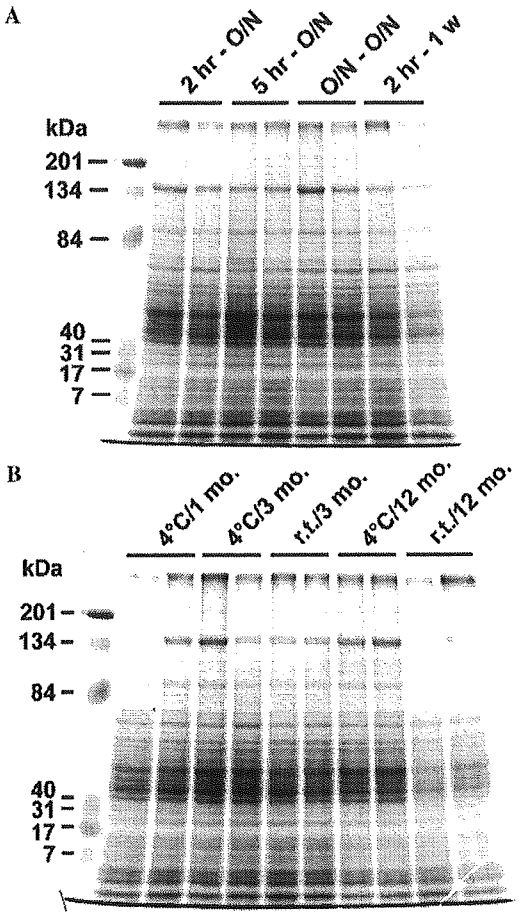

Fig. 4. Integrity of polypeptide bands in protein extracts from methacarn-fixed PETs under different conditions of tissue processing or storage. (A) Experiment 1. (B) Experiment 2.

reduction in the β-actin level was also evident in samples stored for 12 months at 4 °C, but here variability among storage conditions was relatively small, except for the case at room temperature for 12 months, with the CV value of 30.8%. With PCNA, no apparent reduction in protein signals was observed irrespective of the storage condition. For EGFR, a tendency for decrease was observed in samples stored for 3 months at room temperature and 12 months at 4 °C. Storage at room temperature for 12 months was associated with a level only 28% of the value for 1 month at 4 °C.

Discussion

Usually, formaldehyde-based cross-linking agents, such as buffered formalin, limit molecular analysis of DNAs, RNAs, and proteins due to direct interactions with these biomolecules [14]. However, in addition to methacarn, several alternative noncross-linking fixatives, such as HOPE solution [15–17], zinc-based agents [18], acetone-based AMeX [19], and alcohol or alcohol-based fixatives [20,21], have been developed for better preservation of nucleic acids and proteins in PETs. However, information on the effects of tissue processing and storage has hitherto been limited. We here revealed that fixation for a period up to overnight did not affect either the integrity or the expression levels of RNAs and proteins. On the other hand, dehydrating tissues for 1 week did result in slight fluctuations in the relative expression level of both molecular species. Integrity of both total RNAs and polypeptides was retained with storage of PETs at 4 °C but was reduced at room temperature over 12 months. Reflecting the reduction in the integrity, levels of molecules retained after storage at room temperature were also reduced. Reduction was apparent in protein levels by storage for more than 3 months, while this was evident in mRNA levels by 12 months storage.

With regard to the fixation condition in Experiment 1 of the present study, fixation for 5 h resulted in slight reduction in the slc34a2 mRNA level. Although statistical significance was not attained, a similar weak reduction was also noted on another minor mRNA species stx6. However, these reductions lacked apparent time dependency, showing no further reduction by overnight fixation. On the other hand, although most data have not been quantitatively measured and statistically analyzed, tissue fixation with a universal molecular fixative (UMFIX), composed of methanol and polyethylene glycol at a predetermined ratio (Sakura Finetek USA, Inc., Torrance, CA), for 24 h resulted in no obvious changes in either the integrity of extracted total

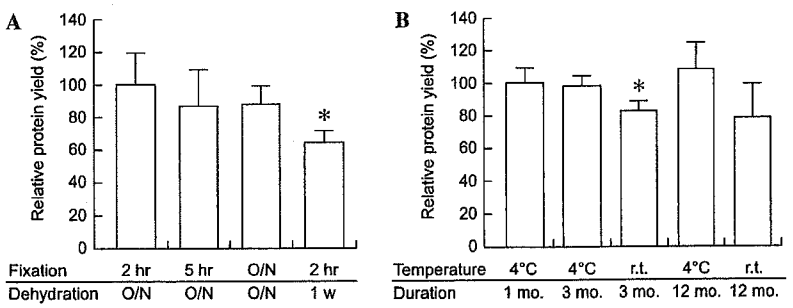

Fig. 5. Relative protein yields from methacarn-fixed PETs under different conditions for tissue processing or storage. (A) Experiment 1 ($n = 3$ for each condition). (B) Experiment 2 ($n = 3$ for each condition). Data are mean ± SD values. *Significantly different from the 2-h-fixed/overnight-dehydrated case in Experiment 1 or from the 1-month-storage case at 4 °C in Experiment 2 ($^*p < 0.05$).

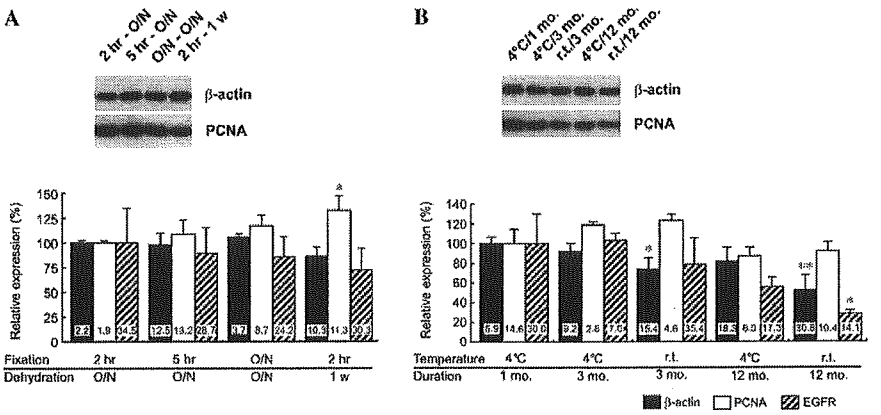

Fig. 6. Relative expression levels of β-actin, PCNA, and EGFR in methacarn-fixed PETs under different conditions of tissue processing or storage. (A) Experiment 1 ($n = 3$ for each condition). (B) Experiment 2 ($n = 3$ for each condition). Data are mean ± SD values and coefficients of variations (CVs). Each inset shows representative blot data for β-actin and PCNA. *, **Significantly different from the 2-h-fixed/overnight-dehydrated case in Experiment 1 or from the 1-month-storage case at 4 °C in Experiment 2 ($^{*}p < 0.05$, $^{**}p < 0.01$).

RNAs or the C_T for detection of GAPDH mRNA levels on real-time RT-PCR analysis, despite slight deterioration of protein signals being evident as compared with the 1-h-fixed case [21]. Taking all the results in combination, fixation with alcohol-based fixatives for more than 24 h may affect protein expression levels, but the effect on mRNA expression may be marginal.

Our findings for dehydration suggest the possibility of release of protein molecules into ethanol solution over time, although levels of nuclear protein PCNA and membrane-bound EGFR were increased (significant) and decreased (nonsignificant), respectively. Lipid extraction by alcohol-based protein precipitating fixatives may result in diffusion artifacts of membrane-bound proteins, causing difficulties with their immunohistochemical detection [22–24]. In our previous study, slight loss of protein yield in methacarn-fixed PETs as compared with UFTs was suggestive of diffusion artifacts [5]. While we observed high variability of EGFR levels among samples as compared with those for PCNA and cytoskeletal β-actin in Experiment 1, this was irrespective of the period of fixation and dehydration. One-week dehydration here also resulted in relative decrease of the mRNA levels of GAPDH and slc34a2, although diffusion artifacts may not have played a role because (i) the yield of total RNA was equivalent to that with other tissue-processing conditions and (ii) the mRNA expression of other genes, CYP2B1 and stx6, was not altered.

With regard to tissue storage effects, RNA degradation was evident in the study using UMFIX-fixed PETs from the visual pattern of major isoforms of ribosomal RNAs, and the cDNA array profile was changed by storage for 4 or 8 weeks at room temperature [21], although the authors argued that the extracted total RNAs were nondegraded and the cDNA array profile was comparable with results for freshly prepared PETs. In the present study, both 18S and 28S ribosomal RNAs mostly disappeared in methacarn-fixed PETs stored for 12 months at room temperature, suggesting degradation over time. On the other hand, mRNA levels in these samples were not entirely affected on measurement with real-time RT-PCR. Usually, real-time PCR utilizes target fragments sized only around 100 bp, and therefore not all RNA molecules in methacarn-fixed PETs are lost on long-term storage at room temperature. Interestingly, this reduction was apparent in mRNA species with low copy numbers, suggesting an uneven effect of long-term storage on degradation of mRNA species, although the corresponding mechanism was unclear.

Integrity of both total RNAs and proteins was well preserved at 4 °C in our study, in accordance with a previous report for the AMeX method, in which only minimal degradation of polypeptides resolved on polyacrylamide gels was documented for a period of 2 years at 4 °C [19]. On the other hand, as with total RNA, decreased intensity of polypeptides in gels was observed with our methacarn-fixed PETs stored for 12 months at room temperature, paralleling the reduced expression levels noted for two of three proteins examined. Oxidation of tissue samples during storage may cause modification of nucleic acids and proteins to affect their yield and integrity [14,25]. In the case of sectioned tissue samples, under ambient conditions they rapidly lose antigenicity; however, the magnitude of this loss differs from antigen to antigen [25]. Variation in the retained expression levels of our three proteins might reflect a similar phenomenon. For tissue sections, combined nitrogen storage and paraffin coating is a useful technique for preserving antigenicity [25]. With regard to storage of PETs, use of vacuum packing is recommended for prevention of oxidation [14]. In the context of tissue storage for future research purposes, vacuum packing may similarly be warranted.

In summary, for gene expression analysis using methacarn-fixed PETs, tissues can be fixed overnight. Moreover, considering similar expression variability among processing conditions, fixed tissues can be kept at the dehydration step for at least 1 week, and PETs can be stored for at least 12 months, but preferably at a temperature of 4 °C in a refrigerator.

Acknowledgments

Dr. Lee was an Awardee of a Postdoctoral Fellowship Program from the Japan Society for the Promotion of Science during the performance of this study. This work was supported by Health and Labour Sciences Research Grants (Risk Analysis Research on Food and Pharmaceuticals) from the Ministry of Health, Labour and Welfare of Japan.

References

[1] M.R. Emmert-Buck, R.F. Bonner, P.D. Smith, R.F. Chuaqui, Z. Zhuang, S.R. Goldstein, R.A. Weiss, L.A. Liotta, Laser capture microdissection, Science 274 (1996) 998–1001.

[2] K. Schütze, G. Lahr, Identification of expressed genes by laser-mediated manipulation of single cells, Nat. Biotechol. 16 (1998) 737–742.

[3] M. Harsch, K. Bendrat, G. Hofmeier, D. Branscheid, A. Niendorf, A new method for histological microdissection utilizing an ultrasonically oscillating needle: demonstrated by differential mRNA expression in human lung carcinoma tissue, Am. J. Pathol. 158 (2001) 1985–1990.

[4] H. Puchtler, F.S. Waldrop, S.N. Meloan, M.S. Terry, H.M. Conner, Methacarn (Methanol-Carnoy) fixation. Practical and theoretical considerations, Histochemie 21 (1970) 97–116.

[5] M. Shibutani, C. Uneyama, K. Miyazaki, K. Toyoda, M. Hirose, Methacarn fixation: a novel tool for analysis of gene expressions in paraffin-embedded tissue specimens, Lab. Invest. 80 (2000) 199–208.

[6] C. Uneyama, M. Shibutani, K. Nakagawa, N. Masutomi, M. Hirose, Methacarn, a fixation tool for multipurpose gene expression analysis from paraffin-embedded tissue materials, Curr. Topics Biochem. Res. 3 (2000) 237–242.

[7] M. Shibutani, C. Uneyama, Methacarn: a fixation tool for multipurpose genetic analysis from paraffin-embedded tissues, in: P.M. Conn (Ed.), Laser Capture Microscopy and Microdissection, Methods Enzymol, vol. 356, Academic Press, London, 2002, pp. 114–125.

[8] C. Uneyama, M. Shibutani, N. Masutomi, H. Takagi, M. Hirose, Methacarn fixation for genomic DNA analysis in microdissected, paraffin-embedded tissue specimens, J. Histochem. Cytochem. 50 (2002) 1237–1245.

[9] H. Takagi, M. Shibutani, N. Kato, H. Fujita, K.-Y. Lee, S. Takigami, K. Mitsumori, M. Hirose, Microdissected region-specific gene expression analysis with methacarn-fixed paraffin-embedded tissues by real-time RT-PCR, J. Histochem. Cytochem. 52 (2004) 903–913.

[10] M. Shibutani, C. Uneyama, Methacarn fixation for genomic DNA analysis in microdissected cells, in: G.I. Murray, S. Curran (Eds.), Laser Capture Microdissection and its Applications, Humana Press, Totowa, Methods Mol. Biol. 293 (2004) 11–25.

[11] J.O. Kim, H.N. Kim, M.H. Hwang, H.I. Shin, S.Y. Kim, R.W. Park, E.Y. Park, I.S. Kim, A.J. van Wijnen, J.L. Stein, J.B. Lian, G.S. Stein, J.Y. Choi, Differential gene expression analysis using paraffin-embedded tissues after laser microdissection, J. Cell. Biochem. 90 (2003) 998–1006.

[12] T.A. Kocarek, J.M. Kraniak, A.B. Reddy, Regulation of rat hepatic cytochrome P450 expression by sterol biosynthesis inhibition: inhibitors of squalene synthase are potent inducers of CYP2B expression in primary cultured rat hepatocytes and rat liver, Mol. Pharmacol. 54 (1998) 474–484.

[13] T.D. Schmittgen, B.A. Zakrajsek, A.G. Mills, V. Gorn, M.J. Singer, M.W. Reed, Quantitative reverse transcription-polymerase chain reaction to study mRNA decay: comparison of endpoint and real-time methods, Anal. Biochem. 285 (2000) 194–204.

[14] M. Srinivasan, D. Sedmak, S. Jewell, Effect of fixatives and tissue processing on the content and integrity of nucleic acids, Am. J. Pathol. 161 (2002) 1961–1971.

[15] J. Olert, K.H. Wiedorn, T. Goldmann, H. Kühl, Y. Mehraein, H. Scherthan, F. Niketeghad, E. Vollmer, A.M. Müller, J. Müller-Navia, HOPE fixation: a novel fixing method and paraffin-embedding technique for human soft tissues, Pathol. Res. Pract. 197 (2001) 823–826.

[16] K.H. Wiedorn, J. Olert, R.A. Stacy, T. Goldmann, H. Kühl, J. Matthus, E. Vollmer, A. Bosse, HOPE—a new fixing technique enables preservation and extraction of high molecular weight DNA and RNA of >20 kb from paraffin-embedded tissues. Hepes–glutamic acid buffer mediated organic solvent protection effect, Pathol. Res. Pract. 198 (2002) 735–740.

[17] U. Uhlig, S. Uhlig, D. Branscheid, P. Zabel, E. Vollmer, T. Goldmann, HOPE technique enables Western blot analysis from paraffin-embedded tissues, Pathol. Res. Pract. 200 (2004) 469–472.

[18] K. Wester, A. Asplund, H. Bäckvall, P. Micke, A. Derveniece, I. Hartmane, P.U. Malmström, F. Pontén, Zinc-based fixative improves preservation of genomic DNA and proteins in histoprocessing of human tissues, Lab. Invest. 83 (2003) 889–899.

[19] Y. Sato, K. Mukai, S. Furuya, T. Kameya, S. Hirohashi, The AMeX method: a multipurpose tissue-processing and paraffin-embedding method. Extraction of protein and application to immunoblotting, Am. J. Pathol. 140 (1992) 775–779.

[20] J.W. Gillespie, C.J. Best, V.E. Bichsel, K.A. Cole, S.F. Greenhut, S.M. Hewitt, M. Ahram, Y.B. Gathright, M.J. Merino, R.L. Strausberg, J.I. Epstein, S.R. Hamilton, G. Gannot, G.V. Baibakova, V.S. Calvert, M.J. Flaig, R.F. Chuaqui, J.C. Herring, J. Pfeifer, E.F. Petricoin, W.M. Linehan, P.H. Duray, G.S. Bova, M.R. Emmert-Buck, Evaluation of non-formalin tissue fixation for molecular profiling studies, Am. J. Pathol. 160 (2002) 449–457.

[21] V. Vincek, M. Nassiri, M. Nadji, A.R. Morales, A tissue fixative that protects macromolecules (DNA, RNA, and protein) and histomorphology in clinical samples, Lab. Invest. 83 (2003) 1427–1435.

[22] B. Gusterson, G. Cowley, J.A. Smith, B. Ozanne, Cellular localisation of human epidermal growth factor receptor, Cell Biol. Int. Rep. 8 (1984) 649–658.

[23] M.A. Judd, K.J. Britten, Tissue preparation for the demonstration of surface antigens by immunoperoxidase techniques, Histochem. J. 14 (1982) 747–753.

[24] B.A. Ponder, M.M. Wilkinson, Inhibition of endogenous tissue alkaline phosphatase with the use of alkaline phosphatase conjugates in immunohistochemistry, J. Histochem. Cytochem. 29 (1981) 981–984.

[25] K.A. DiVito, L.A. Charette, D.L. Rimm, R.L. Camp, Long-term preservation of antigenicity on tissue microarrays, Lab. Invest. 84 (2004) 1071–1078.

TOXICOLOGICAL SCIENCES 90(1), 111–119 (2006)
doi:10.1093/toxsci/kfj076
Advance Access publication December 13, 2005

A Crucial Role of Nrf2 in *In Vivo* Defense against Oxidative Damage by an Environmental Pollutant, Pentachlorophenol

Takashi Umemura,*,[1] Yuichi Kuroiwa,* Yasuki Kitamura,* Yuji Ishii,*,† Keita Kanki,* Yukio Kodama,‡ Ken Itoh,§ Masayuki Yamamoto,§ Akiyoshi Nishikawa,* and Masao Hirose*

*Division of Pathology, National Institute of Health Sciences, 1–18–1, Kamiyoga, Setagaya-ku, Tokyo 158-8501, Japan; †Faculty of Pharmaceutical Science, Department of Analytical Chemistry, Hoshi University, 2–4–41 Ebara, Shinakawa-ku, Tokyo 142-8501, Japan; ‡Division of Toxicology, National Institute of Health Sciences, 1–18–1, Kamiyoga, Setagaya-ku, Tokyo 158-8501, Japan; and §Center for Tsukuba Advanced Research Alliance and Institute of Basic Medical Sciences, University of Tsukuba, Tsukuba, Ibaraki 305-8577, Japan

Received October 7, 2005; accepted November 18, 2005

Our goal was to elucidate roles of Nrf2 in *in vivo* defense against pentachlorophenol (PCP), an environmental pollutant and hepatocarcinogen in mice. We examined oxidative stress and cell proliferation, along with other hepatotoxicological parameters, in the livers of *nrf2*-deficient (wild:+/+, heterozygous:+/−, homozygous:−/−) animals fed PCP in their diet at doses of 0, 150, 300, 600, or 1200 ppm for 4 weeks. For measurement of methoxyresorufin-*O*-demethylase (CYP 1A2), NAD(P):quinone oxidoreductase 1 (NQO1), and UDP-glucuronosyltransferase (UDP-GT), an additional study was performed with all but the 150-ppm dose. Significant elevation of 8-hydroxydeoxyguanosine (8-OH-dG) levels in the liver DNA was observed only in −/− mice treated with PCP at 1200 ppm. Levels of thiobarbituric-acid-reactive substances (TBARS) were also raised significantly compared to those of the relevant +/+ mice. Bromodeoxyuridine labeling indices (BrdU-LIs) of hepatocytes in −/− mice were significantly higher at all doses than those in the relevant +/+ mice. Relative liver weights were unchanged in mice lacking Nrf2, whereas liver weight in +/+ and +/− mice was increased. Significant elevations of serum ALP activity, but not ALT and AST activity, occurred at 600 ppm and above in −/− mice compared to the relevant +/+ mice. Histopathologically, centrilobular hepatocyte necrosis was severe in the −/− mice that received 600 ppm. Although CYP 1A2 activity was elevated in all treated mice, increases in NQO1 levels and UDP-GT activities did not occur only in −/− mice. These data suggest that Nrf2 plays a key role in prevention of PCP-induced oxidative stress and cell proliferation.

Key Words: Nrf2; pentachlorophenol; 8-hydroxydeoxyguanosine; cell proliferation; NQO1.

Chronic exposure to pentachlorophenol (PCP) induces hepatocellular tumors in mice (McConnell *et al.*, 1991), which is of concern, because large amounts of this compound are used as a wood preservative, herbicide, and insecticide, resulting in ubiquitous environmental pollution (Besser, *et al.*, 2005; Dwyer *et al.*, 2005; Masunaga *et al.*, 2001). PCP also has the potential to induce proliferation of hepatocytes and intrahepatic biliary epithelial cells, consequently exerting promotion as well as carcinogenic activity in the liver (Umemura *et al.*, 1999, 2003b). While PCP itself lacks genotoxicity, tetrachlorohydroquione (TCHQ), its major metabolite, has been reported to cause micronuclei and point mutations in V79 hamster cells (Jansson and Jansson, 1991, 1992), presumably contributing to PCP clastogenicity and carcinogenicity. Autooxidation and/or enzymatic oxidation of TCHQ to tetrachlorobenzoquinone (TCBQ) followed by redox cycling gives rise to reactive oxygen species (Naito *et al.*, 1994; Tsai *et al.*, 2001). In fact, we have shown increased 8-hydroxydeoxyguanosine (8-OH-dG) levels in liver DNA of mice given a carcinogenic dose of PCP (Umemura *et al.*, 1996). Also, formation of TCBQ and tetrachlorosemiquinone (TCSQ) adducts results from a direct reaction with DNA during PCP metabolism (Lin *et al.*, 1999, 2002). Thus, information regarding the mode of action underlying PCP hepatocarcinogenesis has accumulated. Questions, however, remain to be clarified regarding *in vivo* preventive mechanisms against phenolic liver carcinogens like PCP, and identification of key factors in *in vivo* defense is clearly necessary for estimation of accurate hazard risk.

Recently, the transcriptional factor Nrf2, which regulates induction of phase 2 and antioxidant enzymes with antioxidant responsive elements (Itoh *et al.*, 1997), has received much attention as a critical role for cellular defense against oxidative stress (Ishii *et al.*, 2000). Given the involvement of NAD(P):quinone oxidoreductase 1 (NQO1) in catalyzing two-electron reduction to detoxify quinones and their derivatives (Ross *et al.*, 2000) in Nrf2-regulated enzymes (Dhakshinamoorthy and Jaiswal, 2001; Nioi *et al.*, 2003; Nioi and Hayes, 2004), it is highly probable that Nrf2 is an important determinant of the hazards with environmental exposure to PCP. Several studies on Nrf2 effects against exogenous chemical exposure have already been demonstrated using *nrf2*-deficient mice, which

[1] To whom correspondence should be addressed. E-mail: umemura@nihs.go.jp.

proved highly susceptible to benzo(*a*)pyrene-induced forestomach (Ramos-Gomez *et al.*, 2003) and *N*-nitrosobutyl (4-hydroxybutyl) amine-induced bladder carcinogenesis (Iida *et al.*, 2004), acetaminophen-hepatotoxicity (Chan *et al.*, 2001; Enomoto *et al.*, 2001) and diesel exhaust–induced lung toxicity (Aoki *et al.*, 2001).

In the present study, to investigate the potential participation of Nrf2 in the biological preventive reaction following PCP exposure, *nrf2*-deficient mice were employed to examine PCP-induced liver lesions in terms of serum biochemistry indicating liver injury, oxidative DNA damage, lipid peroxidation (LPO), and hepatocyte cell proliferation. Particular attention was paid to methoxyresorufin-*O*-demethylase (CYP 1A2) and *Nrf2*-regulating enzymes such as NAD(P):quinone oxidoreductase 1 (NQO1) and UDP-glucuronosyltransferase (UDP-GT).

MATERIALS AND METHODS

Chemicals. PCP (purity, 98.6%) was purchased from Wako Pure Chemical Industries (Osaka, Japan), alkaline phosphatase and bromodeoxyuridine (BrdU) were obtained from Sigma Chemical Co. (St. Louis, MO), and nuclease P1 was from Yamasa Shoyu Co. (Chiba, Japan). Anti-BrdU and anti-NQO1 monoclonal antibodies were from DakoCytomation (Glostrup, Denmark) and Abcam Ltd. (Cambridge, UK), respectively.

Animals, diet and housing conditions. The protocol for this study was approved by the Animal Care and Utilization Committee of the National Institute of Health Sciences. *Nrf2*-deficient mice with an ICR/129SVJ background established by Itoh *et al.* (1997) were crossed with ICR mice (Japan SLC, Schizuoka, Japan); then, homozygous (−/−), heterozygous (+/−), and wild-type littermates (+/+) were obtained from the F1 generation and genotyped by the polymerase chain reaction (PCR) with DNA taken from the tail of each mouse. Mice were housed in polycarbonate cages (five mice per cage) with hard wood chips for bedding in a conventional animal facility maintained under conditions of controlled temperature (23 ± 2°C), humidity (55 ± 5%), air change (12 times per hour), and lighting (12-h light/dark cycle) and given free access to a CRF-1 basal diet (Charles River Japan, Kanagawa, Japan) and tap water.

Animal treatments. Experiment I: A total of 25 7-week-old male mice of each genotype were divided into five groups. PCP was mixed in the basal powder diet at concentrations of 150, 300, 600, and 1200 ppm, and the diets thus prepared were fed to the animals *ad libitum*. The second highest dose was the same as the highest dose in the NTP bioassay, with the purities being a little lower (McConnell *et al.*, 1991). Control mice were similarly fed a basal powder diet (CRF-1). All mice were killed at week 4 by exsanguination under ether anesthesia; blood was collected for measuring serum alkaline phosphatase (ALP), alanine transaminase (ALT), and aspartate aminotransferase (AST) activities from the orbital venous plexus. All mice received BrdU (100 mg/kg) by ip injection once a day for the final 2 days of exposure and once on the final day, 2 h before killing, as previously described (Umemura *et al.*, 1992). At necropsy, the livers were immediately removed and weighed; slices were fixed in buffered formalin for hematoxylin and eosin (H & E) stain or immunohistochemistry for BrdU. Remaining pieces of the livers were frozen with liquid nitrogen and stored at −80°C until measurement of 8-OH-dG in nuclear DNA and levels of thiobarbituric acid-reactive substances (TBARS). Experiment II: A total of 20 7-week-old male mice of each genotype were divided into four groups, and the treatments were performed as in Experiment I, except that the lowest dose was 300 ppm. The livers were similarly sampled and stored for the measurement of CYP1A2 activity, NQO1 protein levels, and UDP-GT activities in the homogenates.

Measurement of nuclear 8-OH-dG. To prevent 8-OH-dG formation as a byproduct during DNA isolation (Kasai, 2002), liver DNA was extracted by a slight modification of the method of Nakae *et al.* (1995). Briefly, nuclear DNA was extracted with a commercially available DNA Extracter WB Kit (Wako Pure Chemical Industries, Ltd.) containing an antioxidant NaI solution to dissolve cellular components. For further prevention of autooxidation in the cell lysis step, deferoxamine mesylate (Sigma Chemical Co.) was added to the lysis buffer (Helbock *et al.*, 1998). The DNA was digested to deoxynucleotides with nuclease P1 and alkaline phosphatase, and levels of 8-OH-dG (8-OH-dG/10^5 deoxyguanosine) were assessed by high-performance liquid chromatography (HPLC) with an electrochemical detection system (Coulochem II, ESA, Bedford, MA).

Measurement of TBARS. Malondialdehyde (MDA, nmol/g) was assessed as an index of lipid peroxidation by the method of Uchiyama and Mihara (1978). In brief, a 0.15-g portion of liver was homogenized with 1.35 ml of 1.15% KCl solution. To 0.05 ml of this homogenate, 0.2 ml 8.1% SDS and 3.0 ml 0.4% 2-thiobarbituric acid in 10% acetic acid solution (pH 3.5) were added, followed by heating in a water bath at 95°C for 60 min. After cooling, 5.0 ml of n-butanol and pyridine (15:1 v/v) and 1.0 ml distilled water were added, and then the mixture was centrifuged at 1,870 × *g* for 10 min. TBARS were measured with a Hitachi F-2500 fluorescence spectrophotometer (Hitachi High-Technologies Co., Tokyo, Japan) at 515 nm (excitation) and 553 nm (emission) in the butanol/pyridine phase.

Immunohistochemical procedures. For immunohistochemical staining of BrdU, sections were treated sequentially with normal horse serum, monoclonal mouse anti-BrdU (1:80), biotin-labeled horse anti-mouse IgG (1:400), and avidin-biotin-peroxidase complex (ABC) after denaturation of DNA with 4 N HCl. The sites of peroxidase binding were demonstrated by incubation with 3,3′-diaminobenzidine tetrahydrochloride (Sigma Chemical Co., St. Louis, MO). The immunostained sections were lightly counterstained with hematoxylin for microscopic examination.

Cell proliferation quantification. For each animal, at least 3000 hepatocytes were counted. The labeling index (LI) was calculated as a percentage value derived from the number of labeled cells divided by the total number of cells counted.

Serum biochemistry. Serum ALP, ALT, and AST levels were measured at SRL Inc. (Tokyo, Japan).

CYP1A2 activity. The livers were homogenized with a Teflon homogenizer in 67 mM phosphate buffer containing 1.15% KCl. The homogenate was centrifuged for 10 min at 10,000 × *g*, 4°C and the resulting supernatant was collected and recentrifuged at 105,000 × *g* for 1 h to obtain microsomal fractions. Protein concentrations were determined with the Advance Protein Assay Reagent (Cytoskeleton Ltd., Denver, CO). The measurement method used in the present study was based on the protocol of McPherson *et al.* (2001). Methoxyresorufin (50 μM, 20 ml) was incubated in triplicate with sample microsomes ±1.25 mM NADPH in 67 mM phosphate buffer, pH 7.4, containing 25 μM $MgCl_2$ for 20 min at 37°C. The reaction was stopped by the addition of ice cold methanol, the precipitate removed by centrifugation, and the fluorescence of the supernatant assessed using excitation (ex) at 530 nm and emission (em) at 585 nm. The formation of resorufin was determined from a standard curve.

Western blotting for NQO1. Liver samples were homogenized with a Teflon homogenizer in ice-cold 50 mM Tris–HCl, pH 7.4 containing 0.25 M sucrose and a 1% protease inhibitor cocktail (Sigma Chemical Co.). The homogenate was centrifuged for 10 min at 10,000 × *g*, 4°C, and the resulting supernatant was collected and recentrifuged at 105,000 × *g* for 1 h to obtain cytosolic fractions. Protein concentrations were determined with a BCA Protein Assay kit (Pierce Biotechnology Ltd., Rockford, IL). Cytosolic fractions containing 20 μg protein were resolved by SDS–PAGE, transferred to Immobilon-P membranes (Millipore Corporation, Bedford, MA), and analyzed with anti-NQO1 (1:1000) (Asher *et al.*, 2002) and anti-β-actin as a loading

control (1:8000, Sigma Chemical Co.). Appropriate peroxidase-conjugated secondary antibodies (1:2000, Dako Cytomation) were used to detect the proteins with ECL Plus (Amersham Bioscience Corp., Piscataway, NJ) reagents.

Microplate UDP-GT assays. Liver samples were homogenized with a Teflon homogenizer in ice-cold 0.1 M Tris–HCl buffer containing 2 mM phenylmethylsulfonyl fluoride, pH 7.8. The homogenate was centrifuged for 20 min at 10,000 × *g*, 4°C, and the resulting supernatant was collected and assessed for protein content with the Advance Protein Assay Reagent (Cytoskeleton Ltd., Denver, CO) before assaying for UGT activity. The measurement method used was based on the protocol of Collier *et al.* (2000). A 96-well microtiter plate containing 30 μl of S9 (1 mg/ml stock), 105 μl of 4-methylumbelliferone (4-MU, Wako) (100 μM, final concentration) in 0.1 M Tris–HCl buffer containing 5 mM $MgCl_2$ and 0.05% BSA, pH 7.4, was placed in a Fluoroskan Ascent FL (Thermo Electron Corp., Waltham, MA) set to read fluorescence at 355-nm ex and 460-nm em. The cofactor uridine 5′- diphosphate glucuronic acid (UDPGA, Sigma) (15 μl, 2 mM final concentration) was added to initiate the reaction. The final volume was 150 μl, and fluorescence was measured every 2 min for 10 min. Results were transformed to nmol/min/mg of protein using a standard curve generated with 4 MU ($\gamma^2 = 0.99$).

Statistics. The significance of differences in the results was evaluated with ANOVA, followed by Dunnett's multiple comparison tests.

RESULTS

Experiment I

As shown in Figure 1, 8-OH-dG levels in the liver DNA of −/− mice at the highest dose were significantly higher than those in the relevant +/+ mice and the control mice. However, there were no changes among any groups of +/+ and +/− mice. Likewise, an increment in the TBARS level was found only in the livers of −/− mice given 1200 ppm, the values being statistically significant as compared with the relevant +/+ mice (Fig. 2). BrdU-LIs for hepatocytes of mice exposed to PCP are shown in Figure 3. A dose-dependent increase was apparent with all of the genotypes, but BrdU-LIs from a dose of 150 ppm in −/− mice and from a dose of 600 ppm in +/− mice were statistically significantly higher compared with the relevant +/+ mice. Figure 4 shows the changes of relative liver weights of *nrf2*-deficient mice given PCP at doses of 0, 150, 300, 600, or 1200 ppm in the diet. In contrast to dose-dependent increases of relative liver weights in both +/+ and +/− mice, there were no changes among −/− mice treated with PCP at doses up to 1200 ppm, each value in the treated −/− mice being significantly lower than that in the relevant +/+ mice. Figure 5 summarizes the changes of serum ALP, ALT, and AST activities of mice treated with PCP at doses of 0, 150, 300, 600, and 1200 ppm in their diet. Significant increments of serum ALP activity occurred at 300 ppm and above in +/− mice as compared with the relevant +/+ mice. ALT and AST activities with all genotypes were increased in a dose-dependent manner, both activities at 1200 ppm in +/− mice being higher with statistical significance as compared with the relevant +/+ mice. Histopathological findings related with PCP treatment are summarized in Table 1. Remarkable cytoplasmic hypertrophy of centrilobular hepatocytes was observed in +/+ and +/− mice given PCP from doses of 150 ppm (Fig. 6A), but this change was much less evident in −/− mice

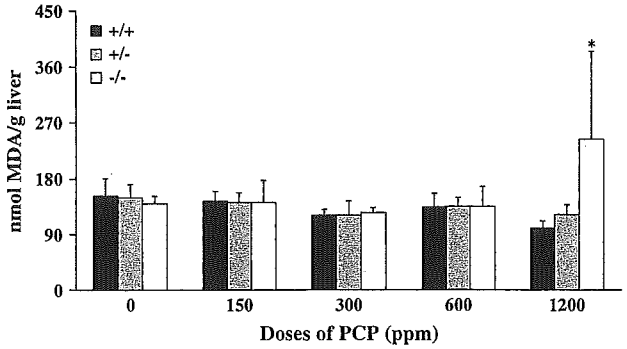

FIG. 2. Changes of TBARS levels in livers of mice fed PCP in the diet at concentrations of 0, 150, 300, 600, or 1200 ppm for 4 weeks. The values are means ± SDs of data for five mice. A significant difference from the relevant +/+ mice is shown by $*p < 0.05$.

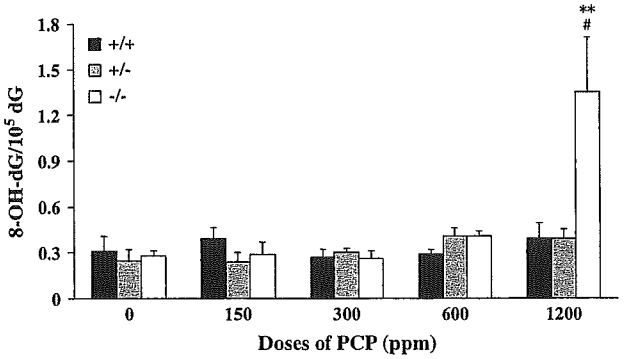

FIG. 1. Changes of 8-OH-dG levels in liver nuclear DNA of mice fed PCP in the diet at concentrations of 0, 150, 300, 600, or 1200 ppm for 4 weeks. The values are means ± SDs of data for five mice. Significant differences from the relevant control (0 ppm) and from the relevant +/+ mice are shown by $\#p < 0.05$ and $**p < 0.01$, respectively.

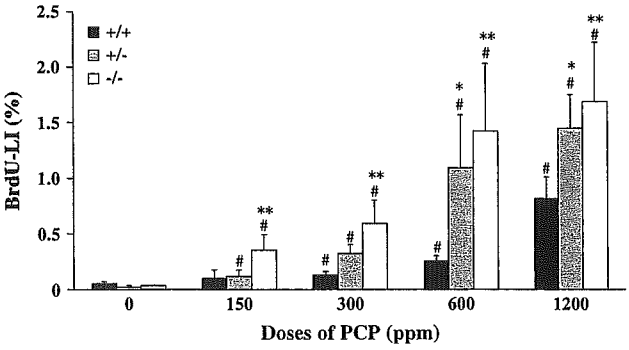

FIG. 3. Changes of BrdU-LIs in hepatocytes of mice fed PCP in the diet at concentrations of 0, 150, 300, 600, or 1200 ppm for 4 weeks. The values are means ± SDs of data for five mice. Significant differences from the relevant control (0 ppm) and from the relevant +/+ mice are shown by $\#p < 0.05$ and $*$,$**p < 0.05$, 0.01, respectively.

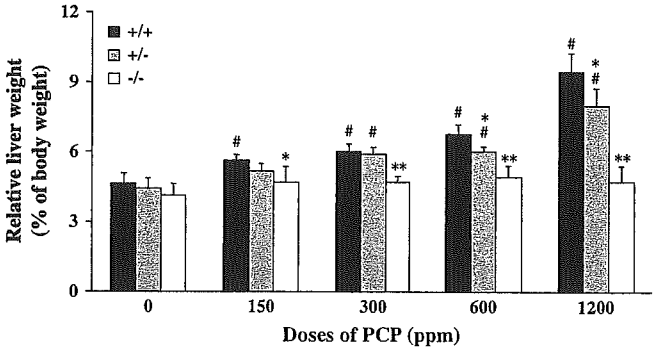

FIG. 4. Changes in relative liver weights for mice fed PCP in the diet at concentrations of 0, 150, 300, 600, or 1200 ppm for 4 weeks. The values are means ± SDs of data for five mice. Significant differences from the relevant control (0 ppm) and from the relevant +/+ mice are shown by #$p < 0.05$ and *,**$p < 0.05$, 0.01, respectively.

(Fig. 6B). Along with hypertrophy, karyomegaly was found at 300 ppm and higher in +/+ and +/− mice (Fig. 6C). In −/− mice, centrilobular hepatocellular necrosis was observed at 600 ppm (Fig. 6D), the severity of which was clearly greater than that in the other genotypes of mice at the same dose (Fig. 6C). At 1200 ppm, ground glass cytoplasm was prominent only in −/− mice (Fig. 6F), there being no changes in terms of the severity of hepatocyte necrosis among the genotypes (Fig. 6E).

Experiment II

Figure 7 illustrates changes in CYP1A2 activity in the livers of mice given PCP at doses of 0, 300, 600, and 1200 ppm in the diet for 4 weeks. Significant elevation of CYP1A2 activity was observed in all of the treated mice, the values in −/− mice at each dose being significantly higher than those in +/+ mice. Western blot analysis using the anti-NQO1 monoclonal antibody demonstrated a dose-related increase in hepatic protein levels in +/+ and +/− mice treated with PCP, in contrast to a lack of the change in −/− mice (Fig. 8A). Quantitation by densitometric scanning and normalization to β-actin levels revealed a statistically significant increase in NQO1 protein levels in the wild-type and heterozygous mice at the highest dose as compared with the relevant control. The levels in −/− mice at any dose were significantly lower as compared with those in the relevant +/+ mice (Fig. 8B). Figure 9 illustrates changes in hepatic UDP-GT activities of mice exposed to PCP at doses of 0, 300, 600, and 1200 ppm in their diet. In the +/+ and +/− cases, activity was elevated from 300 ppm in a dose-dependent manner until 600 ppm. Although the values at 1200 ppm were slightly reduced from the peak, all of the values were statistically significant as compared with the relevant controls. As with the NQO1 protein level, there was no change among the groups of −/− mice, the levels at any doses being statistically lower than those in the relevant +/+ mice.

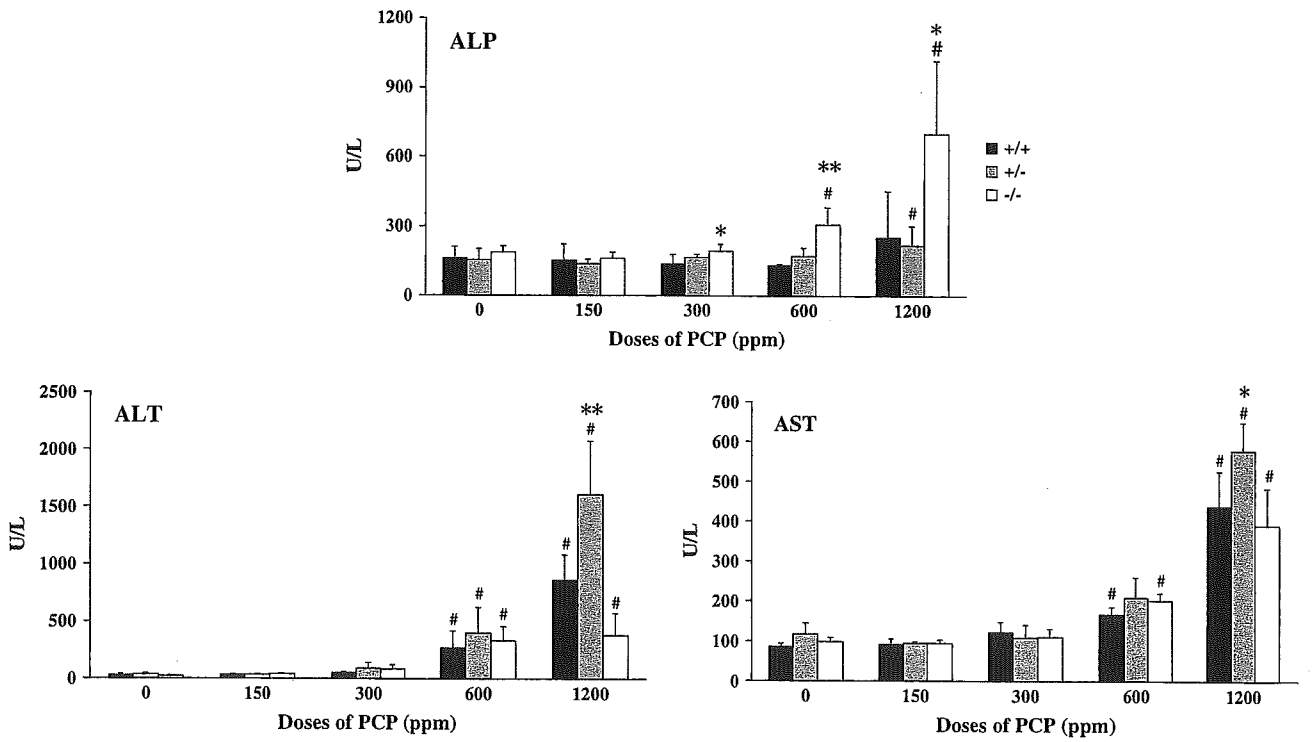

FIG. 5. Changes in serum ALP, ALT, and AST activities in mice fed PCP in the diet at concentrations of 0, 150, 300, 600, or 1200 ppm for 4 weeks. The values are means ± SDs of data for five mice. Significant differences from the relevant control (0 ppm) and from the relevant +/+ mice are shown by #$p < 0.05$ and *,**$p < 0.05$, 0.01, respectively.

TABLE 1
Histopathological Findings for Centrilobular Hepatocytes of *nrf2*-Deficient Mice Given PCP

	0			150			300			600			1200		
PCP (ppm) Finding/Genotype	+/+	+/−	−/−	+/+	+/−	−/−	+/+	+/−	−/−	+/+	+/−	−/−	+/+	+/−	−/−
Cytoplasmic hyperplasia	−	−	−	+	+	−	++	+	±	++	++	±	++	++	±
Ground glass cytoplasm	−	−	−	−	−	−	−	−	−	−	−	−	−	−	++
Karyomegaly	−	−	−	−	−	−	+	+	−	++	++	+	++	++	+
Necrosis	−	−	−	−	−	−	−	−	−	±	±	++	+	+	+

Note. −: negative, ±: slight, +: moderate, ++: severe.

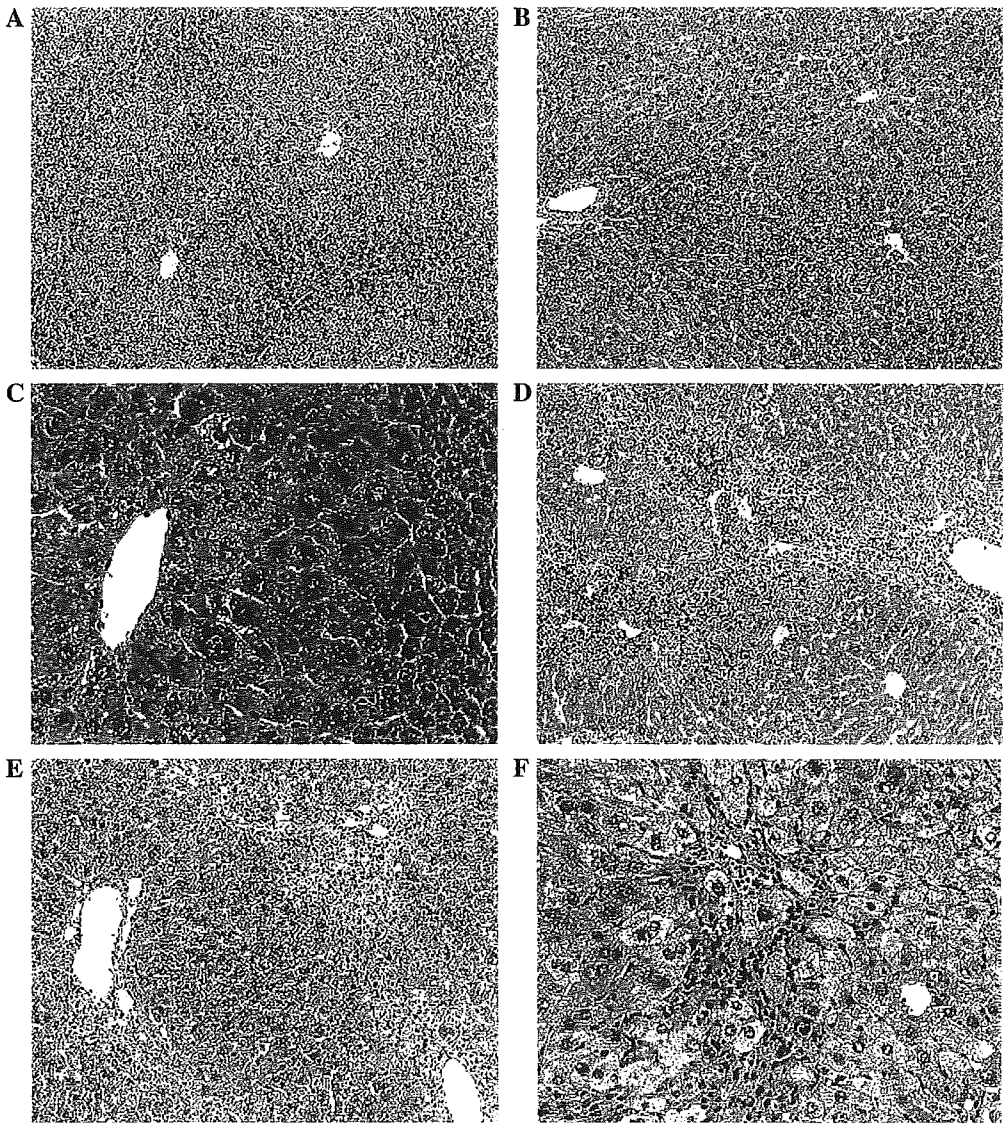

FIG. 6. Photomicrographs of livers of a wild-type mouse (A) and a homozygous *nrf2*-deficient mouse (B) fed PCP at a concentration of 300 ppm for 4 weeks. Note severe centrilobular hypertrophy of hepatocytes (A) and the slight lesion (B). Photomicrographs of livers of a wild-type mouse (C) and a homozygous *nrf2*-deficient mouse (D) fed PCP at a concentration of 600 ppm for 4 weeks. Note severe cytoplasmic hypertrophy with karyomegaly (C) and centrilobular hepatocytes necrosis with inflammatory cell infiltration (D). Photomicrographs of livers of a wild-type mouse (E) and a homozygous *nrf2*-deficient mouse (F) fed PCP at a concentration of 1200 ppm for 4 weeks. Note centrilobular hepatocyte necrosis (E) and ground glass cytoplasm (F).

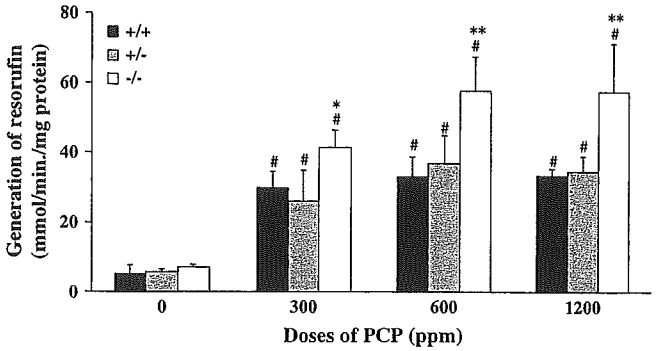

FIG. 7. Changes of CYP1A2 activity in the livers of mice fed PCP in the diet at concentrations of 0, 300, 600, and 1200 ppm for 4 weeks. The values are means ± SDs of data for five mice. Significant differences from the relevant control (0 ppm) and from the relevant +/+ mice are shown by #$p < 0.05$ and *,**$p < 0.05$, $p < 0.01$, respectively.

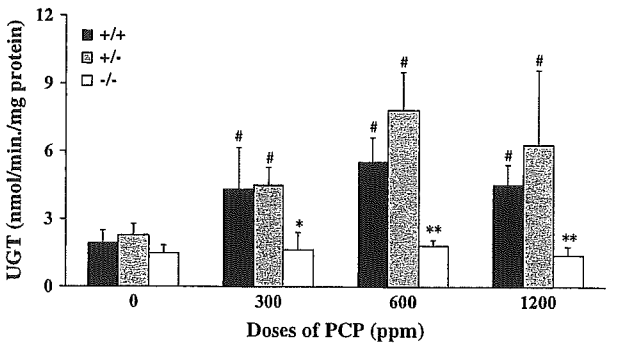

FIG. 9. Changes in UDP-GT activity in livers of mice fed PCP in the diet at concentrations of 0, 150, 300, 600, or 1200 ppm for 4 weeks. The values are means ± SD of data for five mice. Significant differences from the relevant control (0 ppm) and from the relevant +/+ mice are shown by #$p < 0.05$ and *,**$p < 0.05$, 0.01, respectively.

DISCUSSION

The present study showed clear differences in the sensitivity of *nrf2*-deficient and wild-type mice to PCP-induced oxidative stress, consistent with a role for Nrf2 in defense mechanisms. It is in fact well known that a number of proteins that impact oxidative stress, such as heme oxygenase-1 (Alam *et al.*, 1999), peroxiredoxin MSP23 (Ishii *et al.*, 2000), glutamate cysteine ligase (Sekhar *et al.*, 2003), and NQO1 (Nioi *et al.*, 2003), are regulated by Nrf2. Since generation of reactive oxygen species by PCP is considered to occur via its quinone form, we focused specifically on changes in NQO1, by which benzoquinone is supplied with two electrons, consequently skipping the semi-

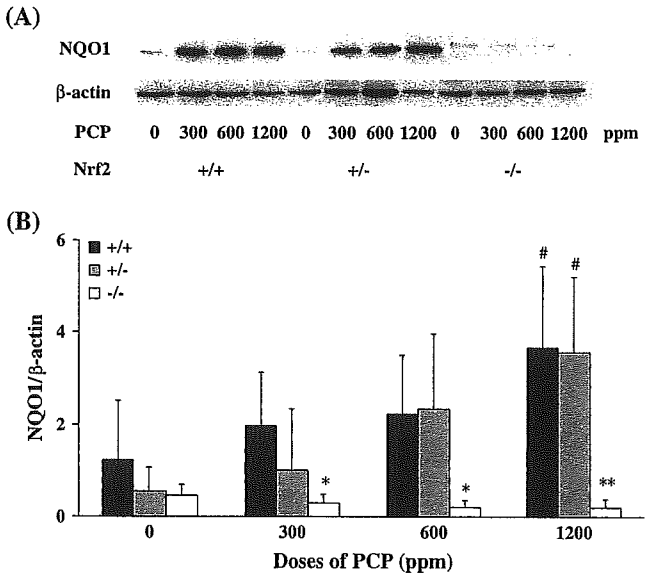

FIG. 8. (A) Western blot analysis of NQO1 from livers of mice fed PCP at concentrations of 0, 300, 600, or 1200 ppm for 4 weeks. (B) Densitometric analysis of Western blot results normalized to β-actin levels in the same tissue sample. The values are means ± SDs of data for five mice. Significant differences from the relevant control (0 ppm) and from the relevant +/+ mice are shown by #$p < 0.05$ and *,**$p < 0.05$, 0.01, respectively.

quinone to form hydroquinone (HQ) (Ross *et al.*, 2000). In fact, in the present study we clearly demonstrated induction of NQO1 by PCP exposure in +/+ and +/− mice, which was completely eliminated in the absence of Nrf2. It is highly probable that NQO1 induced by PCP in +/+ and +/− mice efficiently bypassed TCSQ/TCBQ redox cycling by means of two-electron reduction of TCBQ, subsequently leading to escape from oxidizing DNA base. In turn, no induction of NQO1 following PCP exposure caused DNA base to incur extensive oxidation. Together with our present data on 8-OH-dG formation, in consideration of the ability of both TCSQ and TCBQ to modify bases directly (Lin *et al.*, 1997, 2001), the liver DNA of *nrf2*-deficient mice appears to be in danger of attack by oxidative stress derived from PCP-metabolizing pathways. In an NTP bioassay, PCP at a dose of 600 ppm was hepatocarcinogenic in B6C3F1 mice (McConnell *et al.*, 1991), increases of 8-OH-dG in liver DNA being observed in the same strain with exposure at doses from 300 to 1200 ppm (Umemura *et al.*, 1996). Unexpectedly, there were no changes in 8-OH-dG levels among all of the groups of +/+ and +/− mice in the present study, but their background was 75% ICR. The existence of strain differences among BALB/c, ICR, and C57BL/J mice concerning activities of OGG1 and SOD (Mosquera *et al.*, 2003) might provide an explanation.

Nrf2 is also reported to be a transcriptional factor that regulates enzymes associated with excretion of xenobiotics such as glutathione *S*-transferase and UDP-GT (Thimmulappa *et al.*, 2002). It is generally considered that HQ is subject to glucuronidation and/or sulfation (Siraki *et al.*, 2004), and PCP- and TCHQ-glucuronide conjugations were detected in urine following PCP exposure in rats (Reigner *et al.*, 1991). Our present data pointing to remarkable induction of UDP-GT in +/+ and +/− mice are thus in agreement with PCP toxicokinetics. The activity at a dose of 1200 ppm in either genotype was lower than that at a dose of 600 ppm, albeit the precise rationale was not able to be provided. In consideration of the highest dose being overtly hepatotoxic in +/+ and +/− mice,

the reduction might be secondary to hepatocyte damage, by which the same phenomena observed in the case of the hepatotoxicant, sodium valproate (at a higher dose), was interpreted (Roma-Giannikou *et al.*, 1999). The first step in the metabolism of PCP is to form TCHQ, which is mainly dependent on CYP 1A2 (Ommen *et al.*, 1986), and this was induced with all doses in the present study. There have been no reports indicating a possible role of Nrf2 in regulating P450 isozymes other than CYP 2A5 (Abu-Bakar *et al.*, 2004). Although the further studies on PCP toxicokinetics in B6C3F1 mice demonstrated that sulfation conjugation was predominant in the excretion of PCP (Reigner *et al.*, 1992), our data showing significantly higher levels of CYP1A2 in the treated −/− mice than in their +/+ and +/− counterparts might suggest that the lack of UGT-GT induction results in the higher accumulation of PCP.

PCP has the potential to promote DEN-initiated hepatocarcinogenesis in B6C3F1 mice (Umemura *et al.*, 1999), in line with the increase of BrdU incorporation in hepatocytes (Umemura *et al.*, 2003b). Comparing doses inducing increases of serum ALT activity with those causing elevation of hepatocyte BrdU-LI, we proposed earlier that PCP-induced cell proliferation might result not only from a regenerative response, but also from any other causes, including the alteration of the intranuclear redox status by oxidative stress (Umemura *et al.*, 1996). Likewise, the present results showed that PCP exposure to +/− and −/− mice at all doses, and to +/+ mice at doses of 300 ppm and above was capable of inducing a rise in the BrdU-LI, although a statistically significant elevation of serum biochemical parameters indicating hepatotoxicity first appeared at the dose of 600 ppm. It has been reported that PCP is able to exert inhibitory effects on gap junctional intracellular communication in rat hepatocytes (Sai *et al.*, 1998). In any event, despite the fact that the precise mechanisms underlying PCP-induced cell proliferation are unknown, the present data that BrdU-LIs in −/− mice were significantly higher at any dose than those in the relevant +/+ mice allow us to speculate that a lack of Nrf2 cannot afford to hamper the induction. In view of vulnerability to oxidation of DNA, it can be assumed that *nrf2*-deficient mice are susceptible to PCP-induced hepatocarcinogenicity. To confirm this hypothesis, a carcinogenicity study on PCP using the transgenic mice is now ongoing.

Morphological alteration in the livers of mice exposed to PCP is known to be reflected in marked hepatomegaly (McConnell *et al.*, 1991). In the present study, dose-related increases of relative liver weight occurred in the treated +/+ and +/− mice, which were consistent with histopathological features showing centrilobular hepatocyte hypertrophy. Interestingly, PCP exposure to −/− mice did not affect liver weight or cause severe hepatocyte hypertrophy. Considering the present data that *nrf2*-regulated enzymes were induced by PCP exposure in +/+ and +/− mice, it seems likely that the observed hepatocyte hypertrophy was a consequence of adaptation against xenobiotics. The hypothesis that the hepatomegaly due to PCP exposure has no relation to oxidative stress was supported by our previous findings that coadministration of green tea with PCP was not able to prevent hepatomegaly despite effective suppression of 8-OH-dG formation and hepatocyte proliferation (Umemura *et al.*, 2003a).

The data on serum ALP activities and the histopathological features at a dose of 600 ppm indicated high susceptibility of −/− mice to PCP hepatotoxicity. Nevertheless, the other hepatotoxicological parameters failed to support this finding. The fact that DNA base oxidation and lipid peroxidation did not occur, except in the −/− mice that received high doses, might suggest no link between oxidative stress and hepatotoxicity induced by PCP. Our data showing more induction of CYP1A2 in −/− mice enable us to hypothesize that metabolism of PCP to TCHQ was accelerated in response to accumulated PCP due to a lack of the excretion enzyme. Accordingly, although TCHQ has been considered to play a key role in PCP-induced hepatotoxicity (Wang *et al.*, 2000, 2001), the overall data suggest that PCP itself might be a major cause in the toxicity, with neither TCHQ itself nor oxidative stress derived from the metabolizing pathways of TCHQ as the starting point. However, certain differences in histopathological changes between +/+ and −/− mice strongly imply a necessity for performing further studies to explore the etiology of the hepatotoxicity.

In conclusion, our present data made it clear that Nrf2 exerts preventive effects on oxidative damage and induction of hepatocyte proliferation by PCP, especially with NQO1 playing a key role in *in vivo* defense against these contributing factors to the environmental pollutant-induced carcinogenesis. A single nucleotide polymorphism of NQO1 is known to exist in human populations (Traver *et al.*, 1992, 1997), and data are accumulating that individuals carrying this NQO1 polymorphism have high susceptibility to several cancers (Clairmont *et al.*, 1999; Larson *et al.*, 1999; Schulz *et al.*, 1997; Wiemels *et al.*, 1999). Clearly the carcinogenic risk with environmental exposure to PCP should be considered in this context.

ACKNOWLEDGMENTS

We thank Mss. Machiko Maeda, Ayako Kaneko, and Fukiko Takagi for expert technical assistance in performing the animal experiments and processing histological materials. This work was supported in part by a Grant-in-Aid (12–9) for Cancer Research from the Ministry of Health, Labor and Welfare of Japan.

REFERENCES

Abu-Bakar, A., Satarug, S., Marks, G. C., Lang, M. A., and Moore, M. R. (2004). Acute cadimium chloride administration induces hepatic and renal CYP2A5 mRNA, protein and activity in the mouse: Involvement of transcription factor NRF2. *Toxicol. Lett.* **148,** 199–210.

Alam, J., Stewart, D., Tocuard, C., Boinapally, S., Choi, A. M., and Cook, J. L. (1999). Nrf2, a cCap'nCollar transcription factor, regulates induction of the heme oxygenase-1 gene. *J. Biol. Chem.* **274,** 26071–26078.

Aoki, Y., Nishimura, N., Takahashi, S., Itoh, K., and Yamamoto, M. (2001). Accelerated DNA adduct formation in the lung of the Nrf2 knockout mouse exposed to diesel exhaust. *Toxicol. Appl. Pharmacol.* **173,** 154–160.

Asher, G., Lotem, J., Kama, R., Sachs, L., and Shaul, Y. (2002). NQO1 stabilizes p53 through a distinct pathway. *Proc. Natl. Acad. Sci. U.S.A.* **99,** 3099–3104.

Besser, J. M., Wang, N., Dwyer, F. J., Mayer, F. L., and Ingersoll, C. G. (2005). Assessing contaminant sensitivity of endangered and threatened aquatic species: Part II. Chronic toxicity of copper and pentachlorophenol to two endanger species and two surrogate species. *Arch. Environ. Contam. Toxicol.* **48,** 155–165.

Chan, K., Han, X.-D., and Kan, Y. W. (2001). An important function of Nrf2 in combating oxidative stress: Detoxification of acetaminophen. *Proc. Natl. Acad. Sci. U.S.A.* **98,** 4611–4616.

Clairmont, A., Sies, H., Ramachandran, S., Lear, J. T., Smith, A. G., Bowers, B., Jone, P. W., and Fryer, A. A. (1999). Association of NAD(P)H:quinone oxidoreductase (NQO1) null with numbers of basal cell carcinomas: Use of a multivariate model to rank the relative importance of this polymorphism and those at other relevant loci. *Carcinogenesis* **20,** 1235–1240.

Dhakshinamoorthy, S., and Jaiswal, A. K. (2001). Functional characterization and role of INrf2 in antioxidant response element-mediated expression and antioxidant induction of NAD(P)H:quinone oxidoreductase 1 gene. *Oncogene* **20,** 3906–3917.

Dwyer, F. J., Mayer, F. L., Sappington, L. C., Buckler, D. R., Bridges, C. M., Greer, I. E., Hardesty, D. K., Henke, C. E., Ingresoll, C. G., Kunz, J. L., *et al.* (2005). Assessing contaminant sensitivity of endangered and threatened aquatic species: Part I. Acute toxicity of five chemicals. *Arch. Environ. Contam. Toxicol.* **48,** 143–154.

Enomoto, A., Itoh, K., Nagayoshi, E., Haruta, J., Kimura, T., O'Connor, T., Harada, T., and Yamamoto, M. (2001). High sensitivity of Nrf2 knockout mice to acetaminophen hepatotoxicity associated with decreased expression of ARE-regulated drug metabolizing enzymes and antioxidant genes. *Toxicol. Sci.* **59,** 169–177.

Helbock, H. J., Beckman, K. B., Shigenaga, M. K., Walter, P. B., Woodall, A. A., Yeo, H. C., and Ames, B. N. (1998). DNA oxidation matters: The HPLC-electrochemical detection assay of 8-oxo-deoxyguanosine and 8-oxo-deoxyguanine. *Proc. Natl. Acad. Sci. U.S.A.* **95,** 288–293.

Iida, K., Itoh, K., Kumagai, Y., Oyasu, R., Hattori, K., Kawai, K., Shimazui, T., Akaza, H., and Yamamoto, M. (2004). Nrf2 is essential for the chemopreventive efficacy of oltipraz against urinary bladder carcinogenesis. *Cancer Res.* **64,** 6424–6431.

Ishii, T., Itoh, K., Takahashi, S., Sato, H., Yanagawa, T., Katoh, Y., Bannai, S., and Yamamoto, M. (2000). Transcription factor Nrf2 coordinately regulates a group of oxidative stress-inducible genes in macrophages. *J. Biol. Chem.* **275,** 16023–16029.

Itoh, K., Chiba, T., Takahashi, S., Ishii, T., Igarashi, K., Katoh, Y., Oyake, T., Hayashi, N., Satoh, K., Hatayama, I., *et al.* (1997). An Nrf2/small Maf heterodimer mediates the induction of phase II detoxifying enzymes genes through antioxidant response elements. *Biochem. Biophys. Res. Commun.* **236,** 313–322.

Jansson, K., and Jansson, V. (1991). Induction of mutation in V79 hamster cells by tetrachlorohydroquinone, a metabolite of pentachlorophenol. *Mutat. Res.* **260,** 83–87.

Jansson, K., and Jansson, V. (1992). Induction of micronuclei in V79 hamster cells by tetrachlorohydroquinone, a metabolite of pentachlorophenol. *Mutat. Res.* **279,** 205–208.

Kasai, H. (2002). Chemistry-based studies on oxidative DNA damage: Formation, repair, and mutagenesis. *Free Rad. Biol. Med.* **33,** 450–456.

Larson, R. A., Wang, Y., Banerjee, M., Wiemels, J., Hartford, C., Beau, M. M., and Smith, M. T. (1999). Prevalence of the inactivating 609C-T polymorphism in the NAD(P)H:Quinone oxidoredutase (NQO1) gene in patients with primary and therapy-related myeloid leukemia. *Blood* **94,** 803–807.

Lin, P.-H., La, D. K., Upton, P. B., and Swenberg, J. A. (2002). Analysis of DNA adducts in rats exposed to pentachlorophenol. *Carcinogenesis* **23,** 365–369.

Lin, P.-H., Nakamura, J., Yamaguchi, S., Upton, P. B., La, D. K., and Swenberg, J. A. (2001). Oxidative damage and direct adducts in calf thymus DNA induced by the pentachlorophenol metabolites, tetrachlorohydroquinone and tetrachloro-1,4-benzoquinone. *Carcinogenesis* **22,** 627–634.

Lin, P.-H., Waidyanatha, S., Pollack, G. M., and Rappaport, S. M. (1997). Dosimetry of chlorinated quinone metabolites of pentachlorophenol in the livers of rats and mice based upon measurement of protein adducts. *Toxicol. Appl. Pharmacol.* **145,** 399–408.

Lin, P.-H., Waidyanatha, S., Pollack, G. M., Swenberg, J. A., and Rappaport, S. M. (1999). Dose-specific production of chlorinated quinone and semiquinone adducts in rodent livers following administration of pentachlorophenol. *Toxicol. Sci.* **47,** 126–133.

Masunaga, S., Yano, Y., Ogura, I., Nakai, S., Kanai, Y., Yamamuro, M., and Nakanishi, J. (2001). Identifying sources and mass balance of dioxin pollution in Lake Shinji Basin, Japan. *Environ. Sci. Technol.* **35,** 1967–1973.

McConnell, E. E., Huff, J. E., Hejtmancik, M., Peters, A. C., and Persing, R. (1991). Toxicology and carcinogenesis studies of two grades of pentachlorophenol in B6C3F1 mice. *Fund. Appl. Toxicol.* **17,** 519–532.

McPherson, R. A. C., Tingle, M. D., and Ferguson, L. R. (2001). Contrasting effects of acute and chronic dietary exposure to 2-amino-3-methyl-imidazo[4,5-f]quinoline (IQ) on xenobiotic metabolizing enzymes in the male Fischer 344 rat: Implications for chemoprevention studies. *Eur. J. Nutr.* **40,** 39–47.

Mosquera, D. I., Stedeford, T., Cardozo-Pelaez, F., and Sanchez-Ramos, J. (2003). Strain-specific differences in the expression and activity of OGG1 in the CNS. *Gene Exp.* **11,** 47–53.

Naito, S., Ono, Y., Somiya, Y., Inoue, S., Ito, K., Yamamoto, K., and Kawanishi, S. (1994). Role of active oxygen species in DNA damage by pentachlorophenol metabolites. *Mutat. Res.* **310,** 79–88.

Nakae, D., Mizumoto, Y., Kobayashi, E., Noguchi, O., and Konishi, Y. (1995). Improved genomic/nuclear DNA extraction for 8-hydroxydeoxyguanosine analysis of small amounts of rat liver tissue. *Cancer Lett.* **97,** 233–239.

Nioi, P., Mcmahon, M., Itoh, K., Yamamoto, M., and Hayes, J. D. (2003). Identification of a novel Nrf2-regulated antioxidant response element (ARE) in the mouse NAD(P)H:quinone oxidoredutase 1 gene: Reassessment of the ARE consensus sequence. *Biochem. J.* **374,** 337–348.

Nioi, P., and Hayes, D. (2004). Contribution of NAD(P)H:quinone oxidoreductase 1 to protection against carcinogenesis, and regulation of its gene by the Nrf2 basic-region leucine zipper and the arylhydrocarbon receptor basic helix–loop–helix transcription factors. *Mutat. Res.* **555,** 149–171.

Ommen, B. V., Adang, A., Muller, F., and Van, P. J. (1986). The microsomal metabolism of pentachlorophenol and its covalent binding to protein and DNA. *Chem. Biol. Interact.* **60,** 1–11.

Ramos-Gomez, M., Dolan, P. M., Itoh, K., Yamamoto, M., and Kensler, T. W. (2003). Interactive effects of *nrf2* genotype and oltipraz on benzo[*a*] pyrene-DNA adducts and tumor yield in mice. *Carcinogenesis* **24,** 461–467.

Reigner, B. G., Gungon, R. A., Hoag, M. K., and Tozer, T. N. (1991). Pentachlorophenol toxicokinetics after intravenous and oral administration to rat. *Xenobiotica* **21,** 1547–1558.

Reigner, B. G., Rigod, J. F., and Tozer, T. N. (1992). Disposition, bioavailability, and serum protein binding of pentachlorophenol in the B6C3F1 mouse. *Pharm. Res.* **9,** 1053–1057.

Roma-Giannikou, E., Syriopoulou, V., Kairis, M., Pangali, A., Sarafidou, J., and Constantopoulos, A. (1999). *In vivo* effect of sodium valporate on mouse liver. *Cell. Mol. Life Sci.* **56,** 363–369.

Ross, D., Kepa, J. K., Winski, S. L., Beall, H. D., Anwar, A., and Siegel, D. (2000). NAD(P)H:quinone oxidoreductase 1 (NQO1): Chemoprotection, bioactivation, gene regulation and genetic polymorphisms. *Chem. Biol. Interact.* **129,** 77–97.

Sai, K., Upham, B. L., Kang, K.-S., Hasegawa, R., Inoue, T., and Trosko, J. E. (1998). Inhibitory effect of pentachlorophenol on gap junctional intracellular communication in rat liver epithelial cells *in vitro*. *Cancer Lett.* **130,** 9–17.

Schulz, W. A., Krummeck, A., Rosinger, I., Eickelmann, O., Neuhas, C., Ebert, T., Schmitz-Drager, B., and Sies, H. (1997). Increased frequency of a null allele for NAD(P)H:quinone oxidoredutase (NQO1) gene in patients with urological malignancies. *Pharmacogenetics* **7,** 235–239.

Sekhar, K. R., Crooks, P. A., Sonar, V. N., Friedman, D. B., Chan, J. Y., Meredith, M. J., Starnes, J. H., Kelton, K. R., Summar, S. R., Sasi, S., *et al.* (2003). NADPH oxidase activity is essential for Keap 1/Nrf2-mediated induction of GCLC in response to 2-indol-3-yl-methylenequinuclidin-3-ols. *Cancer Res.* **63,** 5636–5645.

Siraki, A. G., Chan, T. S., and O'Brien, P. J. (2004). Application of quantitative structure-toxicity relationships for the comparison of the cytotoxicity of 14 p-benzoquinone congeners in primary cultured rat hepatocytes versus PC12 cells. *Toxicol Sci.* **81,** 148–159.

Thimmulappa, R. K., Mai, K. H., Srisuma, S., Kensler, T. W., Yamamoto, M., and Biswal, S. (2002). Identification of Nrf2-regulated genes induced by the chemopreventive agent sulforaphane by oligonucleotide microarray. *Cancer Res.* **62,** 5196–5203.

Traver, R. D., Horikoshi, T., Danenberg, K. D., Stadlbauer, T. H. W., Danenberg, P. V., Ross, D., and Gibson, N. W. (1992). NAD(P)H:quinone oxidoreductase gene expression in human colon carcinoma cells: Characterization of a mutation which modulates DT-diaphorase activity and mitomycin sensitivity. *Cancer Res.* **52,** 797–802.

Traver, R. D., Siegel, D., Beall, H. D., Phillips, R. M., Gibson, N. W., Franklin, W. A., and Ross, D. (1997). Characterization of a polymorphism in NAD(P)H:Quinone oxidoredutase (DT-diaphrose). *Br. J. Cancer* **75,** 69–75.

Tsai, C.-H., Lin, P.-H., Waidyanatha, S., and Rappaport, S. M. (2001). Characterization of metabolic activation of pentachlorophenol to quinones and semiquinones in rodent liver. *Chem. Biol. Interact.* **134,** 55–71.

Uchiyama, M., and Mihara, M. (1978). Determination of malonaldehyde precursor in tissue by the thiobarbituric acid test. *Anal. Biochem.* **86,** 271–278.

Umemura, T., Kai, S., Hasegawa, R., Kanki, K., Kitamura, Y., Nishikawa, A., and Hirose, M. (2003a). Prevention of dual promoting effects of pentachlorophenol, an environmental pollutant, on diethylnitrosamine-induced hepato- and cholangiocarcinogenesis in mice by green tea infusion. *Carcinogenesis* **24,** 1105–1109.

Umemura, T., Kai, S., Hasegawa, R., Sai, K., Kurokawa, Y., and Williams, G. M. (1999). Pentachlorophenol (PCP) produces liver oxidative stress and promotes but does not initiate hepatocarcinogenesis in B6C3F1 mice. *Carcinogenesis* **20,** 1115–1120.

Umemura, T., Kodama, Y., Kanki, K., Iatropoulos, M. J., Nishikawa, A., Hirose, M., and Williams, G. M. (2003b). Pentachlorophenol (but not phenobarbital) promotes intrahepatic biliary cysts induced by diethylnitrosamine to cholangio cystic neoplasms in B6C3F1 mice possibly due to oxidative stress. *Toxicol. Pathol.* **31,** 10–13.

Umemura, T., Sai-Kato, K., Takagi, A., Hasegawa, R., and Kurokawa, Y. (1996). Oxidative DNA damage and cell proliferation in the livers of B6C3F1 mice exposed to pentachlorophenol in their diet. *Fundam. Appl. Toxicol.* **30,** 285–289.

Umemura, T., Tokumo, K., and Williams, G. M. (1992). Cell proliferation induced in the kidneys and livers of rats and mice by short term exposure to the carcinogen p-dichlorobenzene. *Arch. Toxicol.* **66,** 503–507.

Wang, Y.-J., Ho, Y.-S., Jeng, J.-H., Su, H.-J., and Lee, C.-C. (2000). Different cell death mechanisms and gene expression in human cells induced by pentachlorophenol and its major metabolite, tetrachlorohydroquinone. *Chem. Biol. Interact.* **128,** 173–188.

Wang, Y.-J., Lee, C.-C., Chang, W.-C., Liou, H.-B., and Ho, Y.-S. (2001). Oxidative stress and liver toxicity in rats and human hepatoma cell line induced by pentachlorophenol and its major metabolite tetrachlorohydroquinone. *Toxicol. Lett.* **122,** 157–169.

Wiemels, J. L., Pagnamenta, A., Taylor, G. M., Eden, O. B., Alexander, F. E., and Greaves, M. F. (1999). A lack of a functional NAD(P)H:quinone oxidoreductase allele is selectively associated with pediatric leukemias that have MLL fusions. *Cancer Res.* **59,** 4095–4099.

Available online at www.sciencedirect.com
SCIENCE DIRECT
ELSEVIER
Archives of Biochemistry and Biophysics 447 (2006) 127–135
ABB
www.elsevier.com/locate/yabbi

Possible involvement of NO-mediated oxidative stress in induction of rat forestomach damage and cell proliferation by combined treatment with catechol and sodium nitrite

Yuji Ishii [a], Takashi Umemura [b,*], Keita Kanki [b], Yuichi Kuroiwa [b], Akiyoshi Nishikawa [b], Rie Ito [a], Koichi Saito [a], Hiroyuki Nakazawa [a], Masao Hirose [b]

[a] *Department of Analytical Chemistry, Hoshi University, 2-4-41 Ebara, Shinagawa-ku, Tokyo 142-8501, Japan*
[b] *Division of Pathology, National Institute of Health Sciences, 1-18-1 Kamiyoga, Setagaya-ku, Tokyo 158-8501, Japan*

Received 15 October 2005, and in revised form 23 January 2006
Available online 17 February 2006

Abstract

To clarify the mechanisms underlying forestomach carcinogenesis in rats by co-treatment with catechol and sodium nitrite ($NaNO_2$), we investigated the involvement of oxidative stress resulting from reaction of the two compounds. Since generation of semiquinone radical, hydroxyl radical (·OH), and peroxynitrite ($ONOO^-$) arose through the reaction of catechol with NO, we proposed that superoxide resulting from catechol oxidation reacted with excess NO, consequently yielding ·OH via $ONOO^-$. Male F344 rats were co-treated with 0.2% catechol in the diet and 0.8% $NaNO_2$ in the drinking water for 2 weeks. Prior to occurrence of histological evidence indicating epithelial injury and hyperplasia, 8-hydroxydeoxyguanosine levels in forestomach epithelium significantly increased from 12 h together with appearance of immunohistochemically nitrotyrosine-positive epithelial cells. There were no remarkable changes in rats given each chemical alone. We conclude that oxidative stress due to NO plays an important role in induction of forestomach epithelial damage, cell proliferation, and thus presumably forestomach carcinogenesis.

Keywords: Catechol; Sodium nitrite; Nitric oxide; Hydroxyl radical; Peroxynitrite; 8-Hydroxydeoxyguanosine; Oxidative stress; Forestomach; Electron spin resonance, Carcinogenesis, Nitrotyrosine

Sodium nitrite ($NaNO_2$)[1] is widely used as a food additive to preserve and tinge color on cured meat and fish [1]. Furthermore, we consume nitrate from exogenous sources such as vegetables and water, some of this being reduced to nitrite in vivo by microflora in the buccal cavity [2]. Catechol is used as a topical antiseptic agent, also being found in cigarette smoke and coffee [3], which implies the risk of human exposure to the two chemicals at the same time. Previously, we reported that treatment with 0.8% catechol in the diet enhanced rat forestomoach and glandular stomoach carcinogenesis in a two-stage carcinogenesis model [4], and induced glandular stomach tumors in rats without prior initiation treatment [5–7]. In addition, combined treatment with 0.2% $NaNO_2$ in the drinking water and 0.8% catechol in the diet induced pronounced hyperplasia in the forestomach epithelium in a 4-week experiment [8]. Moreover, this treatment clearly enhanced *N*-methyl-*N*-nitro-*N*-nitrosoguanidine (MNNG)-initiated forestomach carcinogenesis in rats and also induced forestomach papilloma without initiation [9–11]. The results thus suggested that combined treatment has car-

* Corresponding author. Fax: +81 3 3700 1425.
E-mail address: umemura@nihs.go.jp (T. Umemura).

[1] *Abbreviations used:* $NaNO_2$, sodium nitrite; MNNG, *N*-methyl-*N*-nitro-*N*-nitrosoguanidine; $O_2^{\cdot-}$, superoxide; $ONOO^-$, peroxynitrite; DMPO, 5,5-dimethyl-1-pyrroline-*N*-oxide; NOC-7, 1-hydroxy-2-oxo-3-(*N*-methyl-3-aminoethyl)-3-methyl-1-triazene; 8-OHdG, 8-hydroxydeoxyguanosine; DTPA, diethylenetriaminepentaacetic acid; DHRD, dihydrorhodamine; RD, rhodamine 123; CAT, catalase; SOD, superoxidedismutase; DMF, dimethylformamide.

0003-9861/$ - see front matter © 2006 Elsevier Inc. All rights reserved.
doi:10.1016/j.abb.2006.01.017

cinogenic potential for the rat forestomach. Although the forestomach is a characteristic organ of rodents, not found in man, the possible involvement in carcinogenesis of agents to which humans may be appreciably exposed suggests a necessity of investigating the underlying mechanisms.

$NaNO_2$ readily reacts with reductants to generate nitric oxide (NO) under neutral conditions [12–15]. It has been generally accepted that NO reacts with superoxide ($O_2^{\cdot-}$) to form peroxynitrite ($ONOO^-$), which is a strong oxidizing and nitrating species with multiple potential cytotoxic effects [16–20]. We have shown generation of NO resulting from the reaction of $NaNO_2$ with ascorbic acid in vitro, and a tendency for elevation of 8-hydroxydeoxyguanosine (8-OHdG) levels in DNA of forestomach epithelium of rats after combined treatment [21] in addition to induction of hyperplasia and enhancement of forestomach carcinogenesis [8]. Although catechol is an atomic antioxidant, like ascorbic acid, its reducing ability is considered to be much weaker. Accordingly, it is unlikely that NO is generated by the reaction of catechol with $NaNO_2$, unlike the case with ascorbic acid. However, the fact that NO can be spontaneously produced from $NaNO_2$ under acidic conditions [22,23] allows us to speculate that interaction of NO with catechol might occur in the forestomach of rats given catechol and $NaNO_2$. NO is reported to be effectively eliminated in vitro by incubation with catechol [24], which suggests that NO oxidizes catechol to form quinones, possibly in the presence of oxygen. There is therefore a possibility that coexistence of catechol with NO might give rise to $O_2^{\cdot-}$ by the catechol/quinone redox cycle. In fact, it has already been reported that catechol derivatives such as catechol–estrogen react with NO, producing $O_2^{\cdot-}$ as a consequence [25,26].

The aim of the present study is to explore the mechanisms underlying combined effects of catechol and $NaNO_2$ on forestomach carcinogenesis in rats. In vitro, we identified radicals generated by reaction of catechol and NO, and attempted to elucidate pathways. In an in vivo study, to investigate whether oxidative stress occurs under carcinogenic condition, we measured 8-OHdG levels in forestomach epithelium of rats given catechol and $NaNO_2$ along with histopathological and immunohistochemical examinations.

Materials and methods

Chemicals

$NaNO_2$, catechol, and mannitol were purchased from Wako Pure Chemical Co. (Osaka, Japan). 4-Carboxyphenyl-4,4,5,5-tetramethylimidazoline-1-oxyl-3-oxide (Carboxy-PTIO), 5,5-dimethyl-1-pyrroline-*N*-oxide (DMPO) and 1-hydroxy-2-oxo-3-(*N*-methyl-3-aminoethyl)-3-methyl-1-triazene (NOC-7) were obtained from Dojindo Co. (Kumamoto, Japan). Alkaline phosphatase, diethylenetriaminepentaacetic acid (DTPA), dihydrorhodamine (DHRD), rhodamine 123 (RD), catalase (CAT), and superoxidedismutase (SOD) were from Sigma Chemical Co. (St. Louis, MO), and nuclease P1 was from Yamasa Shoyu Co. (Chiba, Japan). All other chemicals used were of specific analytical or HPLC grade.

ESR conditions

ESR was measured with a spectrometer JEOL JES-FR30 (JEOL, Tokyo, Japan) under the following conditions: magnetic field, 335.0 ± 5 mT; power, 9.0 mW; frequency, 16 GHz; modulation width, 0.063 mT; gain, 500; sweep time, 0.5 min; time constant, 0.03 s.

Analysis of products of catechol reaction with NO by UV–vis absorption spectroscopy

Catechol was incubated in 100 mM sodium phosphate buffer, pH 7.4, containing 1 mM DTPA and 0.1 mM of the NO donor, NOC-7, at room temperature, and the absorption spectra between 500 and 200 nm were recorded at 15-min intervals for up to 60 min, using a Shimadzu UV-1600PC (Kyoto, Japan).

Detection of semiquinone radicals from catechol

Taking advantage of the fact that quinone of catechol was stable in dimethylformamide (DMF) solution [27], the measurement of semiquinone radical was examined in the mixture of 500 mM sodium phosphate buffer (pH7.4) and DMF. One hundred micro liters of 0.1 M catechol (final concentration; 10 mM) was added to 1 mM DTPA containing 500 mM sodium phosphate buffer, pH 7.4, followed by the addition of 500 μL DMF and 50 μL of 10 mM NOC 7 diluted in 10 mM NaOH. This mixture was transferred to a quartz flat cell of 200 μL for ESR measurement after mixing for 1 min. Since semiquinone radical was also generated in alkaline solution [28], the production of semiquinone radical in the solution of catechol with the vehicle of NOC-7 alone was also measured. As a control, the solution of NOC-7/DMF was conducted. All studies were performed at room temperature.

Detection of radical generation using ESR on reaction of catechol with NO with or without SOD and/or CAT

DMPO was used for the detection of radicals. The reaction procedure was as follows: one hundred micro liters of 1 mM catechol was added to 1 mM DTPA containing 100 mM sodium phosphate buffer, pH7.4, followed by the addition of 5 μL DMPO and 100 μL of 1 mM NOC-7. This mixture was transferred to a quartz flat cell of 200 μL for ESR measurement after mixing for 10 min, then ESR spectra were recorded. To investigate the effects of antioxidant enzymes on radical generation, changes in DMPO spectrum intensity by the addition of

10,000 U/mL CAT and/or 1000 U/mL SOD were measured. The signal height was represented as the ratio to that of Mn^{2+} as reference. All studies were performed at room temperature.

Quantification of peroxynitrite by the reaction of catechol and NO

$ONOO^-$ was determined according to the methods of Neil et al. [29] and Benoit et al. [25]. $ONOO^-$ efficiently oxidizes DHRD to form the fluorescence product RD. Thus, $ONOO^-$ formation was assayed by monitoring RD formation at 490 nm. Stock solution of DHRD (28.9 mM) in DMF was stored at −20 °C before use. The reaction solutions consisted of 100 mM sodium phosphate buffer, pH7.4, containing 1 mM DTPA, 3 mM DHRD 100 μM catechol, and 100 μM NOC-7. The total production of $ONOO^-$ was measured at 10-min intervals for up to 60 min after the incubation and the microplate was read at 490 nm. A standard curve was made after the addition of authentic RD. Since ·OH, NO, and NO_2 also oxidize DHRD to RD [29], the production of RD in the solution of DHRD with NOC-7 alone or NOC-7/catechol/mannitol was measured. All studies were performed at room temperature.

Animals, diet, and housing conditions

The protocols for this study were approved by the Animals Care and Utilization Committee of the National Institute of Health Sciences. Five-week-old male F344 rats (specific pathogen-free) were purchased from SLC Japan (Shizuoka, Japan) and housed in polycarbonate cages (three rats per cage) with hardwood chips for bedding in a conventional animal facility maintained under conditions of controlled temperature (23 ± 2 °C), humidity (55 ± 5%), air change (12 times per h), and lighting (12 h light/dark cycle). The animals were given free access to Oriental MF basal diet (Oriental Yeast, Tokyo, Japan) and tap water, and were used after a 1-week acclimation period.

Animal treatments

At the age of 6 weeks, a total of 168 rats were divided into four groups consisting of 42 animals each and treated with basal diet, 0.2% catechol in the diet, 0.8% $NaNO_2$ in the drinking water or 0.8% catechol plus 0.2% $NaNO_2$. They were fasted for 24 h before the chemical treatment and sub-groups were sacrificed after 12, 24 h, 1 and 2 weeks treatment. Since the amount of forestomach epithelium from one animal was too small to allow the examinations planned in the present study, forestomach epithelia were collected as one sample from three animals for 8-OHdG measurement at 12 h and 2 weeks. Forestomachs were excised and their epithelia were collected using razors. Samples were immediately frozen in liquid nitrogen and stored in the deep freezer at −80 °C until measurement of 8-OHdG in nuclear DNA. For histological analysis, three animals each were assessed at each of the points of time examined. The forestomach tissue was fixed in buffered formalin and then routinely processed for embedding in paraffin, sectioning and H&E and immunohistochemical staining.

Measurement of nuclear 8-OHdG

To prevent 8-OHdG formation as a byproduct during DNA isolation, forestomach epithelium DNA were extracted by slight modification of the method of Nakae et al. [30]. Briefly, nuclear DNA was extracted with a commercial DNA isolation kit (DNA extractor WB Kit, Wako Pure Chemical Co, Osaka) containing an antioxidant NaI solution to dissolve cellular components [31]. Because of further prevention against autooxidation in the cell lysis step, deferoxamine mesylate (Sigma Chemical Co, St. Louis, MO) was added to the lysis buffer [32]. After digestion to deoxynucleotides with nuclease P1 and alkaline phosphatase, levels of 8-OHdG (8-OHdG/10^5 deoxyguanosine) were then assessed by high performance liquid chromatography (HPLC) with an electrochemical detection system (Coulochem II, ESA, Bedford, MA).

Immunohistochemical procedures

The slides were incubated in 0.6% H_2O_2 for 30 min at room temperature to block endogenous peroxidase activity. The sections were then blocked with 1% goat serum in PBS for 30 min. After washing with PBS, the sections were incubated overnight with anti-NT rabbit polyclonal IgG (800×) or anti-iNOS rabbit PAb (200×) (BD Transduction Laboratories, San Diego, CA) in 1% bovine serum albumin, in PBS. The next day, the sections were washed with PBS, and a Vector Universal Elite ABC kit (PK-6101) was used according to the manufacturer's instructions. The slides were counterstained with hematoxylin then dehydrated with ethanol and xylene before permanent mounting and microscopic evaluation.

Statistics

For statistical analysis, Student's *t* test or Welch's *t* test were used to compare 8-oxodG levels between groups.

Results

Analysis of products of catechol reaction with NO by UV–vis absorption spectroscopy

As shown in Fig. 1, time-dependent increases of absorption near at 350 nm were observed with mixtures of catechol and NO, attributable to the formation of quinone derivatives of catechol along with decrease near 250 nm.

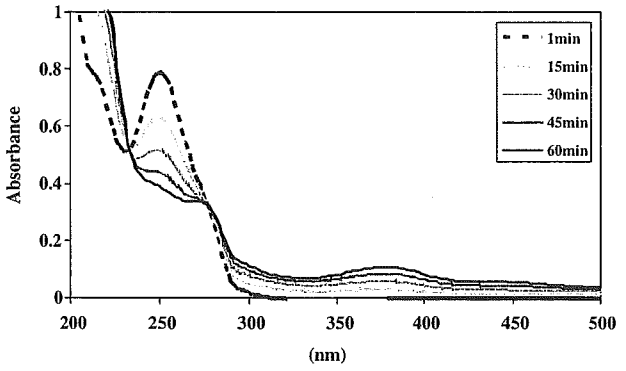

Fig. 1. Changes in absorption spectra of catechol (0.1 mM) incubated with NOC-7 (0.1 mM) for up to 1 h at room temperature in 100 mM sodium phosphate buffer at pH 7.4.

Detection of semiquinone radicals from catechol

Judging from the previous data that a specific ESR spectrum showing semiquinone radical generation was obtained by the reaction of catechol with metal [33], ESR signal observed in the solution of catechol with NOC-7/DMF was presumably originated from semiquinone radical, which was decreased at 30 min possibly due to its instability (Figs. 2A and B). The same ESR signal was slightly observed in the solution of catechol with NaOH, a vehicle of NOC-7 (Figs. 2C), which seems to be resulted from reaction of catechol with alkaline solution [28].

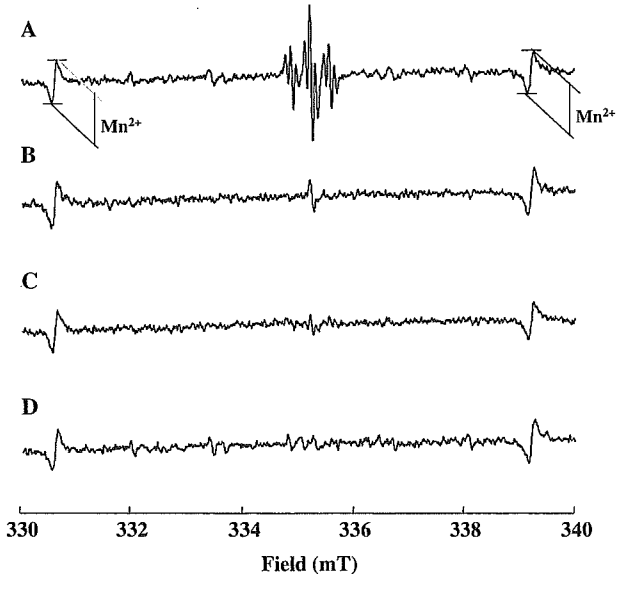

Fig. 2. ESR spectra of semiquinone radicals. Semiquinone radical was generated by the oxidation of 100 mM catechol by 1 mM NOC-7. These reagents were incubated for 1 min (A) and 30 min (B) at room temperature in the mixture of 1 mM DTPA containing 500 mM sodiumm phosphate buffer (pH 7.4) and DMF. ESR spectra of 100 mM catechol/10 mM NaOH (C) or 1 mM NOC-7 alone as a control (D) were measured. These reagents were incubated for 1 min at room temperature in the mixture of 1 mM DTPA containing 500 mM sodium phosphate buffer (pH 7.4) and DMF. Values presented are means ± SD of five separate experiments.

Detection of radical generation using ESR on reaction of catechol with NO with or without SOD and/or CAT

Prior to the analysis, we confirmed the standard spectrum of DMPO with hydroxyl radical (·OH), $O_2^{\cdot-}$ and methyl radical (·CH_3) [34] using by H_2O_2/NaOH/DMSO system (Fig. 3A). The spectrum of 5,5-dimethyl-2-hydroxypyrrolidine-*N*-oxyl (DMPO-OH) was observed with the mixed-solution of 0.1 mM catechol and 0.1 mM NOC-7 in 1 mM DTPA containing 100 mM sodium phosphate buffer at pH 7.4 after mixing for 10 min (Fig. 3B). There were no observations of spectrum by 0.1 mM catechol or 0.1 mM NOC-7 alone (data not shown). Additionally, we examined the effects of SOD and/or CAT on the formation of ·OH in the solution of catechol and NOC-7. Based on the spectrum, Fig. 4 illustrated changes of the signal intensity of DMPO-OH in the mixture of catechol/NOC-7 solution with SOD (1000 U/mL) and/or CAT (10,000 U/mL). The presence of CAT alone did not affect the signal intensity of DMPO-OH derived from the catechol/NOC-7 solution. In contrast to the signal increased in the presence of SOD alone, addition of CAT and SOD effectively eliminated it.

Quantification of peroxynitrite by the reaction of catechol and NO

Fig. 5 shows time-course changes of RD production after the incubation of DHRD with NOC-7 alone, NOC-7/catechol or NOC-7/catechol/mannitol. Production of RD in the solution of DHRD/NOC-7 increased rapidly and reached a maximum level at 10 min, gradually decreasing afterwards and vanishing at 60 min after the start of the reaction. Although RD products in the DHRD/NOC-7/catechol solution increased and decreased in proportion to the changes in the DHRD/NOC-7 solution, the values in the

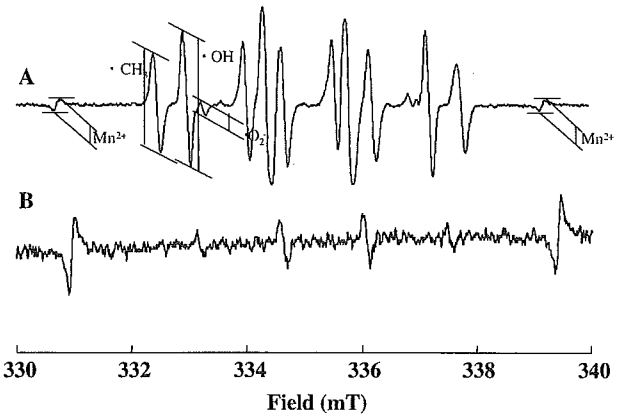

Fig. 3. Typical ESR spectra of DMPO with ·OH, $O_2^{\cdot-}$, and ·CH_3, using the H_2O_2/NaOH/DMSO system (A). ESR spectrum in the reaction of catechol (0.1 mM) incubated with NOC-7 (0.1 mM) at 10 min (B).